Twenty-Seven Tamoxifen-Inducible iCre-Driver Mouse Strains for Eye and Brain, Including Seventeen Carrying a New Inducible-First Constitutive-Ready Allele

Andrea J. Korecki,* Jack W. Hickmott,*,† Siu Ling Lam,* Lisa Dreolini,‡ Anthony Mathelier,*,1 Oliver Baker,§,2 Claudia Kuehne, Russell J. Bonaguro,* Jillian Smith,‡ Chin-Vern Tan,* Michelle Zhou,* Daniel Goldowitz,*,† Jan M. Deussing,** A. Francis Stewart,§ Wyeth W. Wasserman,*,† Robert A. Holt,†,‡,†† and Elizabeth M. Simpson*,†,‡‡,§§,3**

*Centre for Molecular Medicine and Therapeutics at BC Children's Hospital, University of British Columbia, Vancouver, British Columbia V5Z 4H4, Canada, †Department of Medical Genetics, University of British Columbia, Vancouver, British Columbia V6T 1Z3, Canada, ‡Canada's Michael Smith Genome Sciences Centre, British Columbia Cancer Agency, Vancouver, British Columbia V5Z 4S6, Canada, §Genomics, BIOTEC, Center for Molecular and Cellular Bioengineering, Technische Universität Dresden, 01307, Germany, **Max Planck Institute of Psychiatry, Munich 80804, Germany, ††Department of Molecular Biology and Biochemistry, Simon Fraser University, Burnaby, British Columbia V5A 1S6, Canada, ‡‡Department of Ophthalmology and Visual Sciences, University of British Columbia, Vancouver, British Columbia V5Z 3N9, Canada, and §§Department of Psychiatry, University of British Columbia, Vancouver, British Columbia V6T 2A1, Canada,

ORCID IDs: 0000-0003-3764-1138 (J.W.H.); 0000-0001-5127-5459 (A.M.); 0000-0003-2581-6252 (R.J.B.); 0000-0003-4756-4017 (D.G.); 0000-0002-9329-5252 (J.M.D.); 0000-0001-6098-6412 (W.W.W.); 0000-0002-0654-4303 (E.M.S.)

ABSTRACT To understand gene function, the cre/loxP conditional system is the most powerful available for temporal and spatial control of expression in mouse. However, the research community requires more cre recombinase expressing transgenic mouse strains (cre-drivers) that restrict expression to specific cell types. To address these problems, a high-throughput method for large-scale production that produces high-quality results is necessary. Further, endogenous promoters need to be chosen that drive cell type specific expression, or we need to further focus the expression by manipulating the promoter. Here we test the suitability of using knock-ins at the docking site 5′ of *Hprt* for rapid development of numerous cre-driver strains focused on expression in adulthood, using an improved cre tamoxifen inducible allele (icre/ERT2), and testing a novel inducible-first, constitutive-ready allele (icre/f3/ERT2/f3). In addition, we test two types of promoters either to capture an endogenous expression pattern (MaxiPromoters), or to restrict expression further using minimal promoter element(s) designed for expression in restricted cell types (MiniPromoters). We provide new cre-driver mouse strains with applicability for brain and eye research. In addition, we demonstrate the feasibility and applicability of using the locus 5′ of *Hprt* for the rapid generation of substantial numbers of cre-driver strains. We also provide a new inducible-first constitutive-ready allele to further speed cre-driver generation. Finally, all these strains are available to the research community through The Jackson Laboratory.

KEYWORDS gene/expression; retina; cornea; brain; inducible/constitutive; promoter; transgenic mice; *Hprt* locus; targeted mutation; bacterial artificial chromosome

doi: https://doi.org/10.1534/genetics.119.301984
Manuscript received December 20, 2018; accepted for publication February 11, 2019; published Early Online February 14, 2019.
Available freely online through the author-supported open access option.
Supplemental material available at Figshare: https://doi.org/10.25386/genetics.7716308.
[1]Present address: Centre for Molecular Medicine Norway (NCMM), University of Oslo, 0318 Norway.
[2]Present address: King's College London, New Hunt's House, Guy's Campus, SE1 1UL, United Kingdom.
[3]Corresponding author: The Centre for Molecular Medicine and Therapeutics, University of British Columbia, 3020–980 West 28th Ave., Vancouver, BC V5Z 4H4, Canada. E-mail: simpson@cmmt.ubc.ca

TO understand gene function, the cre/loxP conditional system is the most powerful available for temporal and spatial control of expression in mouse (Hoess *et al.* 1986; Bradley *et al.* 2012; Murray *et al.* 2012; Rosen *et al.* 2015; Kaloff *et al.* 2017). Large-scale efforts such as the International Knockout Mouse Consortium (IKMC) have targeted nearly 18,500 genes in mouse embryonic stem cells (ESCs), which have conditional potential in mice, dependent upon inactivation of their alleles by Cre recombinase catalyzing site-specific DNA recombination between 34 bp loxP recognition

sites (Kaloff *et al.* 2017). The IKMC has recently pointed out that "ideally, cre-driver mice should be at hand for every adult cell type to dissect pleiotropic gene functions related to human disease" (Kaloff *et al.* 2017). To that end, for spatial and temporal control of gene inactivation, the research community requires: (1) more cre recombinase expressing transgenic mouse strains (cre-drivers), and (2) cre-drivers that restrict expression to specific cell types.

Temporal control of cre activation can be further increased beyond that of the promoter used by the inclusion of an inducible cre protein such as the tamoxifen responsive cre/ERT2 fusion protein (Indra *et al.* 1999). This inducible system has cre fused to a mutated estrogen receptor (ERT2) such that Cre/ERT2 is normally sequestered in the cytoplasm and inactive, but, when tamoxifen binds ERT2, the cre fusion protein translocates to the nucleus, where it is active (Indra *et al.* 1999). Therefore, the expression pattern of cre from the inducible system reports on a combination of the promoter driving cre, but only during the "window of time" when tamoxifen is present. Inducible alleles have found some application in development, although the toxicity of tamoxifen has been a limitation. However, in adulthood, their application is broad, since tamoxifen toxicity is less of a concern and the reduction in expression complexity, by not reporting on development, is profound. In contrast to the inducible allele, constitutive cre reflects only the promoter used (Zinyk *et al.* 1998). Cre is always present in the nucleus, and thus is a "historical" reporter of any expression from development through adulthood. Such alleles have found substantial application in development, but, since many genes express more broadly in development and become more restricted in adulthood, the final additive labeling in adulthood can be undesirably complex.

A large-scale effort, employing several different strategies, has been underway to produce both inducible and constitutive cre-drivers for use with the IKMC conditional alleles (Murray *et al.* 2012; Rosen *et al.* 2015; Kaloff *et al.* 2017). These span from generation of ESCs only, through animals, to extensively characterized cre-driver strains; the latter being the most immediately valuable to the community. Supporting the usability of these resources by the community is easy access through a repository, including information as to where the resource is, and whether it is held as a mouse strain, alive, or cryopreserved. The mouse genome informatics (MGI) cre portal (www.creportal.org) is a resource that allows researchers to retrieve a list of all recombinase-containing transgenes and knock-in alleles. There are currently 1777 strains of mice listed that are available from an International Mouse Strain Resource (IMSR) repository; this represents strains made from 833 different genes. These strains correspond to 1011 random-insert transgenic and 766 knock-in strains. Of the knock-in strains, 32 are at *Hprt*, 25 at Gt(ROSA), and 57 are enhancer traps. Of these strains, 339 MGI cre alleles are listed in the IMSR as live mice, representing 234 genes.

To address the first problem of generating more cre-driver strains, a high-throughput method of large-scale production that produces high-quality results is necessary. Three strategies were considered for this trial: random insertion, knock-in at the endogenous locus, and a "docking site" in the mouse (Murray *et al.* 2012). The often-used random insertion approach for cre-driver mice generates strains quickly, but is uncontrolled for number of cre transgenes inserted and their location in the genome—both factors that influence the expression of the transgene and necessitate characterization of many strains per construct. More desirable would be a predictable homologous recombination knock-in strategy, so that only one strain need be generated and characterized per construct. Knock-in of a cre transgene in the mouse gene to capture the endogenous expression was very attractive, but before Clustered Regularly Interspaced Short Palindromic Repeats (CRISPR) technology, generating many large homologous recombination constructs, and selecting hundreds of ESC clones, was deemed prohibitively slow and daunting. In addition, this strategy generates a new, possibly deleterious, allele in the very gene whose normal expression is to be captured. Instead, we chose to use one of the two docking sites in the mouse genome; *Gt(ROSA)26Sor* on Chromosome 6 and *Hprt* on the X Chromosome. Although both are ubiquitous genes, the *Gt(ROSA)26Sor* locus is known to drive strong ubiquitous expression (Soriano 1999; Muzumdar *et al.* 2007; Madisen *et al.* 2010), whereas the region 5′ of *Hprt* has been shown to provide a relatively neutral environment in which the expression pattern of the knocked-in promoter is primarily maintained (Farhadi *et al.* 2003; Portales-Casamar *et al.* 2010; Schmouth *et al.* 2013; de Leeuw *et al.* 2014). Critically, this location also remains the only site in the mouse genome for docking bacterial artificial chromosomes (BACs) constructs, even in excess of 200 kb (Schmouth *et al.* 2012b, 2013; Peeters *et al.* 2018). When used with human DNA, the "high-throughput human genes on the X Chromosome" (HuGX) strategy, designed for single copy, site specific, repetitive knock-in of transgenes using an established set of homology arms for constructs (Yang *et al.* 2009), which undergo relatively high-frequency homologous recombination (average 48% of selected clones) (Schmouth *et al.* 2013), was the most attractive for this study.

To address the second problem of generating cre-drivers that restrict expression to specific cell types, endogenous promoters must be chosen that drive such focused expression, or we need to restrict expression further by manipulating the promoter. The average size of a human genomic region per gene is ~150 kb (3×10^6 kb in the genome/~20,000 genes), thus, to capture all regulatory regions for a gene of interest, a "MaxiPromoter" (human BAC with a reporter gene inserted at the start codon) may achieve this. We have previously used this strategy to capture brain and eye expression from the human genes *AMOTL1*, *MAOA*, *NOV*, and *NR2F2* (Schmouth *et al.* 2013). To restrict expression to less than that of the endogenous gene, we have previously used bioinformatic approaches to identify brain and eye-specific regulatory elements to produce "MiniPromoters" (Portales-Casamar *et al.* 2010; de Leeuw *et al.* 2014). Plasmid-based MiniPromoters were designed for

restricted region- and cell-type expression, and to be amenable for use in gene therapy as they are <4 kb and made entirely from human DNA. We have published 45 MiniPromoters driving a reporter by knock-in 5′ of the *Hprt* locus (Portales-Casamar *et al.* 2010; de Leeuw *et al.* 2014), and 33 in recombinant adeno-associated virus (rAAV) (de Leeuw *et al.* 2016; Hickmott *et al.* 2016; Simpson *et al.* 2018). Employing human DNA for promoters relies heavily on conservation of DNA-sequence and expression, and presumably reduces our success when testing in mice. However, it allows us to delineate regions of human DNA in MaxiPromoters needed for expression, and facilitates the design of MiniPromoters, thereby increasing translation to gene therapy.

In this work, we detail the CanEuCre project—a successor of the Pleiades Promoter Project in cooperation with EUCOMMTOOLS and IKMC Projects—in which we address the need for more high quality cell type specific cre-driver mice. Here, we test the suitability of using knock-ins at the docking site 5′ of *Hprt* for rapid development of numerous cre-driver strains focused on expression at adulthood, using a previously characterized improved cre (icre) tamoxifen inducible allele (icre/ERT2) (Erdmann *et al.* 2007), and testing a novel inducible-first, constitutive-ready allele (icre/f3/ERT2/f3) so that constitutive expression can also be studied. In addition, we test two types of promoters either to capture an endogenous expression pattern (MaxiPromoters) or to restrict expression further using minimal promoter element(s) designed for expression in restricted cell types (MiniPromoters). In the process, we have added to the mouse strain collection by developing 27 icre-driver strains for the brain and eye, available through The Jackson Laboratory. These 27 strains represent 10 MaxiPromoter strains driving icre/ERT2, 14 MiniPromoter strains driving icre/f3/ERT2/f3, and three control strains driving icre/f3/ERT2/f3. All strains were characterized by RT-PCR, with two inducible MaxiPromoter strains chosen for detailed characterization by histology, and four inducible and constitutive MiniPromoter strains chosen for detailed characterization by histology.

Materials and Methods

MaxiPromoter design and retrofitting

The BAC constructs came from the RPCI-11 human male BAC library (https://bacpacresources.org (Table 1). BACs were modified by two sequential steps of retrofitting using the lambda recombination system (Yu *et al.* 2000). The first retrofitting step allowed the insertion of *Hprt* homologous recombination targeting arms as we have described previously (Schmouth *et al.* 2013). The second step allowed the insertion of the reporter cassette icre/ERT2 at the ATG encoding start codon of the specified gene. Two 50 bp oligonucleotide recombination arms were designed for the insertion of the reporter. The left arm targeted immediately upstream of the endogenous ATG-encoding start codon. Ideally, the right arm targeted immediately after the end of the same exon. Because of sequence composition challenges for retrofitting, in some cases the right arm oligonucleotides designs were altered to target further downstream. For the reporter cassette (pEMS1725), an icre/ERT2 sequence (1983 bp) was designed using a previously published icre sequence (Shimshek *et al.* 2002), a three-amino-acid linker sequence (Metzger and Feil 1999), and an ERT2 sequence (Feil *et al.* 1997). The retrofitting of the reporter cassette was done as we have described previously (Schmouth *et al.* 2013). Briefly, the reporter cassette was designed to contain a kanamycin gene, allowing the selection of correctly retrofitted clones. This resistance gene was designed with flanking full *frt* sites (Lyznik *et al.* 1993), which were used to excise the kanamycin gene via induction of Flp recombinase (Schlake and Bode 1994; Anastassiadis *et al.* 2009). The entire icre/ERT2 cassette, including targeting arms, was sequence verified for each construct.

MiniPromoter design and cloning

MiniPromoter bioinformatics has been described in detail previously (Portales-Casamar *et al.* 2010; de Leeuw *et al.* 2016). The MiniPromoter backbone plasmid (pEMS2001) was produced by three sequential steps. First, we had a new plasmid synthesized (pEMS1925) building on pJ344 (DNA2.0, Menlo Park, CA) and containing: *I-Sce*I (for linearization), *Bam*HI, an insulator (Sakurai *et al.* 2010), a multiple cloning site for introduction of promoters (*Avr*II, *Fse*I, *Mlu*I, and *Asc*I), an intron (optimized chimeric (pCI; Promega, Madison, MI)), icre/ERT2 (with frt-f3 sites flanking the estrogen receptor sequences), a WPRE (Zanta-Boussif *et al.* 2009), a SV40 polyadenylation [poly(A)] signal, another insulator, *Eco*RI, and *Sal*I. Second, the mouse 5′ *Hprt* homology arm (Portales-Casamar *et al.* 2010) was isolated from Pleiades plasmid (pEMS1314) and introduced into pEMS1925 using *Bam*HI. Finally, the human *HPRT* complementary sequence (Portales-Casamar *et al.* 2010) and mouse 3′ *Hprt* arm (Portales-Casamar *et al.* 2010) were isolated from Pleiades plasmid (pEMS1314) and introduced using *Eco*RI/*Sal*I to produce the final pEMS2001. MiniPromoters were generated by direct synthesis (DNA2.0), or isolated from previous Pleiades Promoter plasmids (Portales-Casamar *et al.* 2010; de Leeuw *et al.* 2014, 2016), and cloned into the multiple cloning site of pEMS2001. All new DNA junctions, whether for the reporter cassette, *Hprt* arms, or MiniPromoters, were sequence verified.

Mouse strain generation, husbandry, and breeding

The new mouse strains were generated using a variation of the previously described strategy to insert constructs 5′ of *Hprt* on the mouse X Chromosome (Bronson *et al.* 1996; Heaney *et al.* 2004; Yang *et al.* 2009; Schmouth *et al.* 2013). Briefly, either MaxiPromoter DNA was purified using the Nucleobond BAC 100 kit (Clontech laboratories, Mountain View, CA), or MiniPromoter DNA was purified using the Qiagen MiniPrep kit (Qiagen, Hilden, Germany), and both MaxiPromoters and MiniPromoters were linearized with *I-Sce*I. The constructs were then electroporated into ESCs using the following

Table 1 Ten novel *Hprt* targeted human MaxiPromoter strains generated

Chosen for	Gene	Ple	Parental BAC (RP11-)	BAC size (bp)	Retrofit-ted BAC (bEMS)	Targeted ESC line (mEMS)	Strain name (B6.Cg-)	JAX Stock #
Thalamus	*SLITRK6*	252	398A22	197,372	168	5708[a]	*Hprt*$^{tm340(Ple252\text{-}icre/ERT2)Ems}$	023685
Basal ganglia	*AGTR1*	270	487M24	231,190	237	5930[b]	*Hprt*$^{tm343(Ple270\text{-}icre/ERT2)Ems}$	023688
Blood brain barrier	*CLDN5*	272	16C10	197,627	191	5806[a]	*Hprt*$^{tm332\ (Ple272\text{-}icre/ERT2)Ems}$	023677
PvH	*CRH*	274	1006F7	205,667	192	5758[a]	*Hprt*$^{tm353\ (Ple274\text{-}icre/ERT2)Ems}$	023698
Cortex	*HTR1B*	277	990K4	196,504	228	5794[a]	*Hprt*$^{tm335\ (Ple277\text{-}icre/ERT2)Ems}$	023680
Striatum	*KCNA4*	278	63H13	191,783	240	6120[b]	*Hprt*$^{tm357\ (Ple278\text{-}icre/ERT2)Ems}$	023702
Hippocampus	*NEUROD6*	281	1087H14	209,931	193	5724[a]	*Hprt*$^{tm333\ (Ple281\text{-}icre/ERT2)Ems}$	023678
Hippocampus	*NPY2R*	283	937K11	188,618	241	5899[b]	*Hprt*$^{tm354\ (Ple283\text{-}icre/ERT2)Ems}$	023699
Neural stem cells	*SOX3*	286	1019M14	208,479	244	5931[b]	*Hprt*$^{tm355\ (Ple286\text{-}icre/ERT2)Ems}$	023700
Hypoxia	*SPRY1*	287	1126D8	209,197	248	6107[a]	*Hprt*$^{tm358\ (Ple287\text{-}icre/ERT2)Ems}$	023703

BAC, bacterial artificial chromosome; bEMS, BAC Elizabeth M. Simpson; ESC, embryonic stem cell; JAX, The Jackson Laboratory; mEMS, mammalian cell line Elizabeth M. Simpson; Ple, Pleiades promoter; PvH, paraventricular hypothalamic nucleus.
[a] mEMS4857 was the parental ESC line.
[b] mEMS4855 was the parental ESC line.

conditions: voltage, 190 V (MaxiPromoter), 270 V (MiniPromoter); capacitance, 500 μF (MaxiPromoter), 50 μF (MiniPromoter); resistance, 350 ohms (both); using a BTX ECM 630 Electro cell manipulator (BTX, San Diego, CA) (Schmouth *et al.* 2013). A male ESC line from a C57BL/6NTac-$A^{w\text{-}j}/A^{w\text{-}j}$, $Hprt^{b\text{-}m3}$/Y mouse (mEMS4855 or mEMS4857) was used. The agouti gene originated from JAX stock 00051 (C57BL/6J-$A^{w\text{-}j}$/J) and was backcrossed onto C57BL/6NTac (B6/NTac; Taconic, Hudson, NY) for four generations. The *Hprt* gene originated from JAX stock 002171 (B6.129P2-$Hprt^{b\text{-}m3}$/J) and was backcrossed to B6/NTac for six generations. Following the backcrossing to B6/NTac, the agouti and *Hprt* strains were intercrossed for four generations to produce the final ESC line from a generation-equivalent NE4.75F4 mouse blastocyst. ESC derivation and culture was conducted as described previously (Yang *et al.* 2009). Targeted ESC clones were selected in hypoxanthine aminopterin thymidine (HAT) medium, isolated, expanded, frozen, and DNA purified. Human-specific PCR assays were designed and used to initially screen the ESC clones, and verify the integrity of the MaxiPromoter and MiniPromoter inserted in the mouse genome (Yang *et al.* 2009; Schmouth *et al.* 2013). A minimum of three correctly targeted ESC clones per construct were microinjected into C57BL/6J blastocysts (B6/J, JAX Stock 000664) to generate chimeras that were subsequently bred to B6/J females to obtain female germline offspring. A mixed background of B6/NTac and B6/J is designated B6.

A typical breeding strategy is detailed in Supplemental Material, Figure S1. To produce tm#a (#, stands for all numbers in the collection) strains for histology, N1 or N2 females were bred to the 129-ROSA-Stop-tdTomato cre reporter strain (JAX Stock 007914 (minimum N1 backcrossed to 129S1/SvImJ (129, JAX Stock 002448))) to generate both male and female hybrid B6129F1 mice that carried both the icre/ERT2 and ROSA-Stop-tdTomato alleles. One exception was Ple274 (*CRH*) mice, which were bred to B6/J-ROSA-Stop-tdTomato cre reporter strain (JAX Stock 007905) to generate both male and female B6/J mice that carried both the icre/ERT2 and ROSA-Stop-tdTomato alleles. To produce tm#b strains for histology, N1 or N2 females were bred to the B6/J-CAG-flpo strain (MMRRC Stock 032247-UCD)—a germline deleter used to remove the ERT2 portion of the allele. Following this, tm#b females were bred to the 129-ROSA-Stop-tdTomato reporter strain to generate both male and female adult hybrid B6129F1 mice that carried both the icre and ROSA-Stop-tdTomato alleles. As a tm#a control, the UBC (human ubiquitin C) promoter driving cre/ERT2 strain was used (Ruzankina *et al.* 2007). As a tm#b control, the ACTB promoter driving cre strain was used (JAX Stock 003376).

Mice were maintained in the pathogen-free Centre for Molecular Medicine and Therapeutics mouse facility on a 7 AM–8 PM light cycle, 20 ± 2° with 50 ± 5% relative humidity, and had food and water *ad libitum*. All procedures involving mice were in accordance with the Canadian Council on Animal Care and UBC Animal Care Committee (Protocol A10-0267 and A10-0268). Ple274 (*CRH*) mice were also maintained in the Technische Universität Dresden facility on a 12 AM–12 PM light cycle, 22 ± 1° with 55 ± 5% relative humidity, and had food and water *ad libitum*. All procedures involving mice were in accordance with the Guide of the Care and Use of Laboratory Animals of the Government of Bavaria, Germany.

RT-PCR

A minimum of three N2 male mice were used for each strain for RT-PCR experiments. Male N2 mice of at least 6 weeks of age were killed by cervical dislocation; brain and eyes were dissected and rapidly frozen in liquid nitrogen. The brain dissection was into seven regions: olfactory bulbs, telencephalon (without the hippocampus), hippocampus, diencephalon, midbrain, hindbrain (without the cerebellum), and cerebellum. Two to three regions were chosen for each strain. RNA was extracted using the PerfectPure RNA Cell & Tissue kit (5 Prime, Hilden, Germany) and converted to cDNA using the SuperScript III First-Strand Synthesis (Thermo Fisher Scientific, Waltham, MA). For MaxiPromoter strains, assays were designed within ERT2 and for each specific BAC. For

MiniPromoter strains, assays were designed within ERT2, ERT2 to WPRE, and for each specific promoter expect Promoterless, CAGGS, and Ple198, where specific promoter designs were not possible.

Tamoxifen induction

Adult mice were fed a diet of either tamoxifen (TD.120629; Harlan Laboratories, Madison, WI) or no-tamoxifen (control, TD.07570) food for a period of 4 weeks. Following this period, mice were put back on a regular diet for 3 weeks before harvest. Adult Ple274 (*CRH*) mice were fed a diet of tamoxifen (LAS CRdiet CreActive TAM400; LASvendi GmbH, Soest, Germany) during postnatal weeks 10–12. Following this period, mice were put back on a regular diet for 2 weeks before harvest.

Histology—TdTomato epifluorescence and immunofluorescence

Mostly, mice were killed by avertin (MilliporeSigma, Burlington, MA) overdose, and transcardially perfused for 2 min with 1× phosphate-buffered saline (PBS), and 10 min with 4% paraformaldehyde (PFA) in PBS buffer at a flow rate of 5 ml/min. Tissues were removed, postfixed for 2 hr in 4% PFA at 4°, and then cryoprotected with 25% sucrose overnight at 4°. Tissues were then embedded in optimal cutting temperature compound (OCT) on dry ice, and 20 μm cryosections were directly mounted onto slides. For Ple274 (*CRH*), mice were killed by isoflurane (Floren; Abbott, Lake Bluff, IL) overdose, and transcardially perfused for 1 min with 1× PBS, 5 min with 4% PFA (w/v) in PBS, pH 7.4, and 1 min with PBS at a flow rate of 10 ml/min. Brains were removed and postfixed overnight in 4% PFA in 1× PBS at 4°. Brains were washed with 1× PBS and embedded in agarose (Invitrogen, Carlsbad, CA) in PBS, and 50 μm coronal sections were prepared using a vibratome (MICROM HM 650V; ThermoScientific).

Mostly, TdTomato epifluorescence was visualized using an Olympus BX61 fluorescent microscope (Olympus, Tokyo, Japan). Images were processed using Image J (http://rsbweb.nih.gov/ij/), Photoshop, and Illustrator (Adobe, San Jose, CA). For Ple274 (CRH), TdTomato epifluorescence was visualized using a Zeiss Axioplan2 fluorescent microscope (Zeiss, Oberkochen, Germany). Images were digitalized using AxioVision Rel 4.5, and processed using Photoshop and Illustrator.

For immunofluorescent staining, sections were blocked in PBS + 0.4% Triton X-100 (A2058; MilliporeSigma) + 0.3% bovine serum albumin (T8787; MilliporeSigma) for 20 min, and incubated in primary antibody at 4° overnight. Primary antibodies used were anti-CLDN5 (35-2500; Thermo Fisher Scientific), anti-PCP2 (sc-68356; Santa Cruz Biotechnology, Dallas, TX), anti-POU4F1 (also known as anti-BRN3A, sc-8429; Santa Cruz Biotechnology), anti-GAD65/67 (AB1511; MilliporeSigma), anti-TH (MAB318; MilliporeSigma), anti-calretinin (AB1550; Millipore Sigma), and anti-SOX9 (AB5535; MilliporeSigma). Slides were washed 3× with PBS + 0.4% Triton X-100 and incubated with secondary antibody and Hoechst 33342 for 2 h at room temperature. Secondary antibodies used were from Thermo Fisher Scientific: anti-mouse IgG (A11029), anti-rabbit IgG (A11034), and anti-goat IgG (A21222). Sections were washed 3× in 0.1 M phosphate buffer (PB) buffer, 1× in 0.01 M PB buffer, mounted in ProLong Gold (P36930; Thermo Fisher Scientific) and coverslipped. Z-stack images were taken on an TCS SP8 Super-Resolution Confocal Microscope (Leica Microsystems, Wetzlar, Germany), deconvolved using Huygens Professional (Scientific Volume Imaging, Hilversum, Netherlands), and processed as described above. Images with only partial Hoechst overlay were processed as previously described (Hickmott *et al.* 2016). For POU4F1, GAD65/67, TH, and calretinin imaging, antigen retrieval was performed as follows: sections were incubated in citrate acid buffer + 0.05% Tween20 (BP337; Thermo Fisher Scientific), pH 6 for 40 min at room temperature, sections in buffer were then heated to 54° for 20 min before immunofluorescent staining was performed as described above.

Histology—double in situ hybridization

Mice were killed by isoflurane (Floren) overdose. Brains were carefully removed and rapidly frozen on dry ice and 20 μm at −20° coronal sections were prepared using a cryostat (Thermo Fisher Scientific). The sections were thaw mounted onto slides, dried, and kept at −80°. Double *in situ* hybridization (ISH) was performed as previously described (Refojo *et al.* 2011). The following riboprobes were used: *Crh* (3′ UTR): 2108–2370 bp of AY128673; tdTomato: 740–1428 bp of AY678269.

Data availability

Plasmids used for cloning, controls, and Pleiades MiniPromoters are available to the research community through Addgene (www.addgene.org). Mouse strains are available through The Jackson Laboratory (www.jax.org/jax-mice-and-services). The authors affirm that all data necessary for confirming the conclusions of the article are present within the article, figures, and tables. Supplemental material available at Figshare: https://doi.org/10.25386/genetics.7716308.

Results

Ten MaxiPromoter strains –icre/ERT2 (inducible)

Therapeutically interesting regions and cell types of the brain and eye were identified as described in Table 1 and below for selected lines, and 11 genes that had not previously been used for inducible strain development, and with restricted expression that included those cells, were chosen. Human BACs were selected based on coverage of the gene of interest and inclusion of candidate regulatory regions. The ideal BAC covered the entire gene (transcribed genomic region) up to, but not including, the promoter regions of neighboring genes. If multiple suitable BACs were available, priority was

given to the one that included the longest upstream sequence for the chosen gene, to maximize inclusion of relevant regulatory regions. Greater detail for each MaxiPromoter can be found by searching the parental BAC name (Table 1) on the University of California Santa Cruz (UCSC) genome browser (http://genome.ucsc.edu/, accessed February 4, 2019). For each gene, the parental BAC was retrofitted, targeted into a mouse C57BL/6N embryonic stem cell line, and the resulting line was used to successfully derive 10 mouse strains, which were assigned a JAX name and stock number (Table 1).

Figure 1A depicts in more detail our HuGX two-step BAC retrofitting process (Schmouth *et al.* 2013). First, *Hprt* homology arms were inserted into the BAC vector backbone, to allow for homologous recombination targeting immediately 5′ of the *Hprt* gene on the mouse X Chromosome. Second, an icre (Shimshek *et al.* 2002) fused to ERT2 (Feil *et al.* 1997) cassette with a stop codon was inserted at the ATG-encoding start codon of the human gene. Thus, the resulting MaxiPromoter construct contained a reporter gene under the influence of the human regulatory regions of the specified gene. Importantly, no exogenous poly(A) signal was added, so that ideally splicing would continue to the natural 3′ untranslated region and poly(A) signal. The new MaxiPromoter alleles are named, for example, B6.Cg-*Hprt*$^{tm340(Ple253\text{-}icre/ERT2)Ems}$, indicating the insertion is at the *Hprt* mouse gene, is targeted mutation (tm) number 340 generated by the Simpson laboratory (Ems), and contains (shown in brackets) the Pleaides promoter (Ple) number 253 driving icre/ERT2 (Table 1).

Figure 1B depicts the resulting MaxiPromoter strains for histological expression analysis. First, the MaxiPromoter-icre/ERT2 strains were crossed to mice that carried the cre-reporter allele *Gt(ROSA)26Sor*$^{tm14(CAG\text{-}tdTomato)Hze}$, for brevity called ROSA-stop-tdTomato because it contains the ubiquitous ROSA promoter driving a loxP/stop/loxP-tdTomato. Then, the resulting adult offspring carrying both alleles were fed tamoxifen food, or no-tamoxifen control food. Tamoxifen results in the iCre/ERT2 protein, which is normally sequestered in the cytoplasm, entering the nucleus to remove the stop, allowing ROSA driven tdTomato expression. Thus, only cells that expressed icre driven by the restricted MaxiPromoter at the time of adult tamoxifen exposure showed tdTomato expression.

It was important to demonstrate that our icre-reporting system for histological analysis of inducible alleles was able to report on widespread expression throughout the target tissues, and thus would properly reflect the expression of the restricted promoters. Therefore, we crossed mice carrying the UBC-cre/ERT2 ubiquitously expressing inducible allele to the cre-reporter strain ROSA-stop-tdTomato, and adult offspring carrying both alleles were fed tamoxifen, or no-tamoxifen, food. Figure S2A shows that, for example, with tamoxifen, tdTomato epifluorescence was observed in many cells throughout all layers of the retina, and the endothelial and stromal layers of the cornea. However, with no tamoxifen, only occasional positive cells, or groups of cells, were observed in the retina and cornea.

17 MiniPromoter strains—icre/f3/ERT2/f3 (inducible-first constitutive-ready)

The 17 MiniPromoter strains included 14 MiniPromoters selected for therapeutically interesting regions and cell types of the brain and eye as described in Table 2 and below for selected lines, plus three controls. The MiniPromoters chosen for further restricted expression were all tested here for the first time in the mouse genome driving icre. They were a combination of 10 unaltered previously successful designs (Portales-Casamar *et al.* 2010; de Leeuw *et al.* 2014, 2016), one new cut down of a previous design (de Leeuw *et al.* 2014, 2016), and two designs taken directly from the literature (Visel *et al.* 2007; Ariza-Cosano *et al.* 2012; de Leeuw *et al.* 2016). Table S1 details the design sources and any previous publication, including previous MiniPromoter characterization, for each promoter.

The 10 unaltered MiniPromoters were designed previously (Portales-Casamar *et al.* 2010; de Leeuw *et al.* 2014, 2016). Briefly, candidate regulatory regions were selected based on sequence conservation, experimental data provided in the UCSC Genome Browser, and a manual review of the scientific literature. Also included in this set were two controls: Promoterless, with nothing cloned into the promoter location; and CAGGS, a ubiquitous promoter (de Leeuw *et al.* 2016).

The cut down MiniPromoter Ple265 (*PCP2*) was designed based on Ple155 (*PCP2*), which we had previously shown able to deliver lacZ and/or EmGFP expression in bipolar ON cells of the mouse retina, as well as Purkinje cells of the cerebellum (de Leeuw *et al.* 2014, 2016). The original Ple155 was designed by concatenating two *cis*-regulatory human regions (Prom1, 986 bp on the sense strand of *PCP2*, and Prom2, 666 bp on the antisense strand of the *PCP2*) associated with the two known transcription start sites (TSSs) of the two isoforms of the *PCP2* gene (NM_174895 and NM_001271830), respectively. For the new Ple265 design, we hypothesized that the observed eye expression could be driven independently by one of these two promoter regions. We exploited the availability of genome-wide cap-analysis of gene expression (CAGE) data for >800 human cell samples from the FANTOM5 consortium to assess this hypothesis (Arner *et al.* 2015). We found that the Prom1 *cis*-regulatory region harbored two subregions of active TSSs, associated with distinct expression in the testis and in the eye. A similar analysis of the Prom2 *cis*-regulatory region highlighted a single region of active TSSs associated with expression in the brain, mainly the cerebellum. To test if one of these *cis*-regulatory regions could drive specific expression in the eye only, we designed a new MiniPromoter, Ple265, which is 60% the size of Ple155, and composed exclusively of the Prom1 sequence.

The two literature designs were chosen from the VISTA enhancer project, the main goal of which is to identify distant-acting noncoding regulatory elements that drive developmental gene expression in a region-specific manner (Visel *et al.* 2007). Generally, VISTA enhancers are identified using

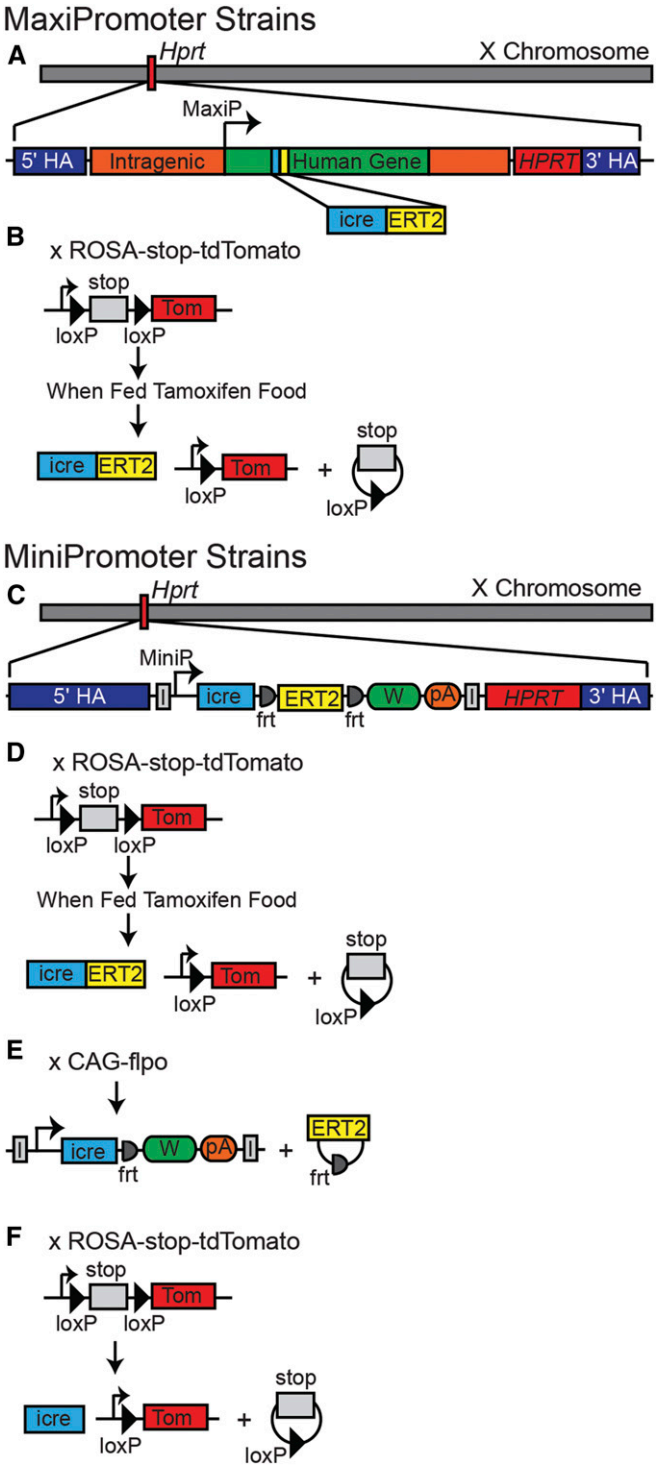

Figure 1 MaxiPromoters (inducible) and MiniPromoters (inducible-first constitutive-ready). (A) MaxiPromoter inducible alleles were constructed by first inserting into a selected human bacterial artificial chromosome (BAC), *Hprt* homology arms and human *HPRT* coding sequence in the vector backbone, and then icre (improved cre)/ERT2 (mutant estrogen receptor) fusion cassette at the ATG encoding start codon of the human gene. Homologous recombination of the modified BAC at the mouse $Hprt^{b\text{-}m3}$ deleted allele resulted in insertion of the MaxiPromoter driving icre/ERT2 immediately 5′ of *Hprt* and "correction" of the *Hprt* deletion ($Hprt^{tm\#}$). (B) Icre expression was histologically characterized by crossing the MaxiPromoter strain to the ROSA-stop-tdTomato strain and adult offspring carrying both alleles being fed tamoxifen-containing food so that the iCre/ERT2 protein recombined the loxP sites, removed the stop, and allowed ROSA driven tdTomato expression. (C) MiniPromoter inducible-first constitutive-ready alleles (tm#a) were constructed in plasmids with insulators (I) surrounding the expression cassette, a MiniPromoter driving icre/ERT2 with f3 sites surrounding ERT2 (icre/f3/ERT2/f3), WPRE transcriptional stabilization element, SV40 poly(A), *Hprt* homology arms, and human *HPRT* coding sequence. As in (A), homologous recombination of the plasmid at the mouse $Hprt^{b\text{-}m3}$ deleted allele resulted in insertion of the MiniPromoter driving icre/ERT2 immediately 5′ of *Hprt* and "correction" of the *Hprt* deletion ($Hprt^{tm\#a}$). (D) As in (B), icre expression was characterized by crossing the MiniPromoter strain (tm#a) to the ROSA-stop-tdTomato strain and adult offspring being fed tamoxifen. The iCre/ERT2 protein recombined the loxP sites, which allowed ROSA driven tdTomato expression. (E) MiniPromoter constitutive alleles (tm#b) were generated by crossing the MiniPromoter tm#a strain to the CAG-flpo deleter strain, which recombined the f3 sites in the germline and removed ERT2 ($Hprt^{tm\#b}$). (F) Similar to (B and D), icre expression was characterized by crossing the MiniPromoter strain (tm#b) to the ROSA-stop-tdTomato strain, but with this constitutive allele, testing required no tamoxifen. The iCre protein recombined the loxP sites, which allowed ROSA-driven tdTomato expression.

extreme evolutionary sequence conservation and/or chromatin immunoprecipitation sequencing (ChIP-seq) data, and then tested in combination with a mouse minimal promoter, *Hspa1a* (aka Hsp68) (Visel *et al.* 2007). We selected two such VISTA enhancers, one each for the forebrain and midbrain. Also included in this set was one control; the VISTA minimal promoter alone (*Hspa1a*).

Originally, 18 MiniPromoters were selected and cloned into our plasmid backbone (except Promoterless), targeted into a mouse C57BL/6N embryonic stem cell line, and the resulting line was used to successfully derive the 17 mouse strains, which were assigned a JAX name and stock number (Table 2).

Figure 1C depicts in more detail the MiniPromoter cloning process. First we generated a plasmid backbone (pEMS2001) that contained: a mouse 5′ *Hprt* homology arm (Portales-Casamar *et al.* 2010); a multiple cloning site for introduction of MiniPromoters; icre fused to ERT2, with f3 sites flanking the ERT2 (Schlake and Bode 1994; Feil *et al.* 1997; Shimshek *et al.* 2002); woodchuck hepatitis virus post-transcriptional regulatory element (WPRE) mut6 version, which abolishes WPRE internal transcriptional activities (Zanta-Boussif *et al.* 2009); an SV40 poly(A) signal; a human *HPRT* complimentary sequence (Portales-Casamar *et al.* 2010); and a mouse 3′ *Hprt* homology arm (Portales-Casamar *et al.* 2010). The expression cassette was also flanked by insulators (Sakurai *et al.* 2010); 5′ of the MiniPromoter and 3′ of the poly(A) signal. The insulators were designed to minimize "site of insertion" genomic effects on the relatively small MiniPromoters, compared to the BAC MaxiPromoters. MiniPromoters were cloned 5′ of the reporter cassette.

For the new icre/f3/ERT2/f3 allele (tm#a), one f3 site was introduced into the spacer between cre and the ERT2 domain, without interrupting the reading frame or changing the spacer length. Another f3 was placed 3′ of the ERT2 stop codon so

Table 2 17 novel *Hprt* targeted MiniPromoter strains generated

Chosen for	Gene/genomic region	Ple	MiniP size (bp)	Plasmid name (pEMS)	Targeted ESC line (mEMS)	Strain name (B6.Cg-)	JAX Stock #
Raphe nuclei	*FEV*	67	2202	2011	6017[a]	*Hprt*$^{tm366a(Ple67icre/ERT2)Ems}$	023711
Gabaergic neurons	*GPR88*	94	3049	2014	6029[a]	*Hprt*$^{tm359a(Ple94-icre/ERT2)Ems}$	023704
Purkinje, bipolar	*PCP2*	155	1652	2004	5985[a]	*Hprt*$^{tm347a(Ple155-icre/ERT2)Ems}$	023692
Raphe nuclei	*SLC6A4*	198	2826	2015	6044[a]	*Hprt*$^{tm351a(Ple198-icre/ERT2)Ems}$	023696
Thalamus	*TNNT1*	232	1209	2010	6006[a]	*Hprt*$^{tm350a(Ple232-icre/ERT2)Ems}$	023695
Cortex	*C8ORF46*	251	2453	2002	5937[a]	*Hprt*$^{tm367a(Ple251-icre/ERT2)Ems}$	023712
Substantia nigra	*PITX3*	253	2484	2003	5929[a]	*Hprt*$^{tm360a(Ple253-icre/ERT2)Ems}$	023705
Neurogenic, müller glia	*NR2E1*	264	3026	2006	6004[b]	*Hprt*$^{tm346a(Ple264-icre/ERT2)Ems}$	023691
Bipolar	*PCP2*	265	986	2005	5991[a]	*Hprt*$^{tm348a(Ple265-icre/ERT2)Ems}$	023693
Glia, astrocytes	*S100B*	266	2982	2007	5950[a]	*Hprt*$^{tm365a(Ple266-icre/ERT2)Ems}$	023710
Glia, oligodendroglia	*UGT8*	267	3014	2009	5970[a]	*Hprt*$^{tm361a(Ple267-icre/ERT2)Ems}$	023706
Glia, oligodendroglia	*OLIG1*	304	2596	2018	6089[a]	*Hprt*$^{tm362a(Ple304-icre/ERT2)Ems}$	023707
Forebrain	hs671[c]	N/AP	2129	2016	6068[a]	*Hprt*$^{tm349a(hs671-icre/ERT2)Ems}$	023694
Midbrain	hs1218[c]	N/AP	2338	2017	6070[a]	*Hprt*$^{tm363a(hs1218-icre/ERT2)Ems}$	023708
Minimal promoter control	*Hspa1a*[c,d]	N/AP	878	2012	6051[a]	*Hprt*$^{tm352a(Hspa1a-icre/ERT2)Ems}$	023697
Ubiquitous control	CAGGS	N/AP	1723	2013	6096[a]	*Hprt*$^{tm364a(CAGGS-icre/ERT2)Ems}$	023709
Promoterless control	(none)	N/AP	0	2001	5895[a]	*Hprt*$^{tm345a(icre/ERT2)Ems}$	023690

ESC, embryonic stem cell; JAX, The Jackson Laboratory; mEMS, mammalian cell lines Elizabeth M. Simpson; MiniP, MiniPromoter; N/AP, not applicable; pEMS, plasmid Elizabeth M. Simpson; Ple, Pleiades promoter.
[a] mEMS4855 was the parental ESC line.
[b] mEMS4857 was the parental ESC line.
[c] Genomic regions from the VISA Enhancer Project (https://enhancer.lbl.gov/).
[d] Synonym Hsp68.

that recombination between the two f3 sites by Flp recombinase will delete the ERT2 domain and bring a new stop codon to the icre open reading frame, resulting in the constitutive allele (tm#b). The new MiniPromoter alleles are named, for example B6.Cg-*Hprt*$^{tm366a(Ple67-icre/ERT2)Ems}$, indicating the insertion is at the *Hprt* mouse gene, is targeted mutation (tm) number 366 generated by the Simpson laboratory (Ems), is the inducible-first constitutive-ready allele (a), and contains (shown in brackets) the Pleaides promoter (Ple) number 67 driving icre/ERT2 (Table 2).

Figure 1D depicts the resulting MiniPromoter tm#a strains for histological expression analysis. MiniPromoter-icre/f3/ERT2/f3 strains were crossed to ROSA-stop-tdTomato, and the resulting adult offspring carrying both alleles were fed tamoxifen, or no-tamoxifen control food. TdTomato expression was then observed in cells that expressed icre driven by the MiniPromoter at the time of adult tamoxifen exposure. Figure 1E depicts the production of MiniPromoter constitutive tm#b strains. The MiniPromoter-icre/f3/ERT2/f3 strains were crossed to mice that carried the germline flp-deleter allele Tg(CAG-flpo)1Afst/Mmucd, for brevity called CAG-flpo because it contains the ubiquitous CAG promoter driving a codon-optimized flippase recombinase (flpo) (Raymond and Soriano 2007), resulting in the recombination of the frt-f3 sites to remove the ERT2. Figure 1F depicts the resulting MiniPromoter tm#b strains for histological expression analysis. MiniPromoter-icre strains were crossed to ROSA-stop-tdTomato resulting in the recombination of the loxP sites to remove the stop. TdTomato expression was then observed in all the cells that had expressed icre driven by the MiniPromoter during either development and/or adulthood.

Again, we demonstrate that our icre-reporting system, used for histological analysis of both inducible and constitutive expression, was able to report on widespread expression throughout the target tissues. For inducible expression, the same UBC-cre/ERT2 controls were used as detailed for MaxiPromoters above (Figure S2A). For constitutive expression, we crossed mice carrying the ACTB-cre ubiquitously expressing allele to the cre-reporter strain ROSA-stop-tdTomato, and analyzed adult offspring carrying both alleles. Figure S2B shows, for example, that tdTomato epifluorescence was observed in many cells throughout most layers of the retina, and in the epithelial, endothelial, and stromal layers of the cornea. We also analyzed adult mice carrying only the ROSA-stop-tdTomato allele. Figure S2C shows that without a cre allele, no tdTomato epifluorescence was observed.

All 27 icre strains showed expression by RT- PCR

Each MaxiPromoter and MiniPromoter strain should be producing icre transcripts dependent upon the respective promoter, but independent of icre protein status (conditional or constitutive). Therefore, for each of the 27 strains, two to three brain regions, or the eye, were chosen based on where expression was expected, harvested from N2 male mice, and assessed by semiquantitative RT-PCR (Table 3). All tissues were positive, with the band intensity being consistent across tissues for a single strain, but with a range of intensities by strain. MaxiPromoter strains showed variable strong, weak, and very weak RT-PCR bands, whereas all MiniPromoter mice showed strong bands. Of particular note was the unexpected strong transcription observed for the MiniPromoter control strain bearing no promoter (none, aka Promoterless).

Table 3 Summary of semi-quantitative RT-PCR results for the 27 strains developed

Ple	Gene/genomic region	Regions tested	RT-PCR results	Chosen for detailed characterization
252	*SLITRK6*	Telenceph (w/o hipp), Hipp, Diencephalon	Weak	No
270	*AGTR1*	Telenceph (w/o hipp), Hipp, Diencephalon	Weak	No
272	*CLDN5*	Olfactory Bulb, CB	Strong	Yes; see Figure 2 and Table 4
274	*CRH*	Olfactory Bulb, Telenceph (w/o hipp), Hindbrain (w/o CB)	Very weak	Yes; see Figure 3 and Table 4
277	*HTR1B*	Telenceph (w/o hipp), CB	Very weak	No
278	*KCNA4*	Olfactory Bulb, Telencephalon, Diencephalon	Strong	No
281	*NEUROD6*	Cortex, Hipp	Strong	No
283	*NPY2R*	Telenceph (w/o hipp), Hipp, Diencephalon	Strong	No
286	*SOX3*	Olfactory Bulb, Telencephalon, Hipp	Strong	No
287	*SPRY1*	Olfactory Bulb, Telencephalon, Hipp	Strong	No
67	*FEV*	Diencephalon, Midbrain, Hindbrain (w/o CB)	Strong	No
94	*GPR88*	Telenceph (w/o hipp), Hipp, Diencephalon	Strong	No
155	*PCP2*	Eyes, Diencephalon, CB	Strong	Yes; see Figure 4 and Table 4
198	*SLC6A4*	Olfactory Bulb, Diencephalon, Hindbrain (w/o CB)	Strong	Yes; see Figure 6 and Table 4
232	*TNNT1*	Hipp, Diencephalon, Hindbrain (w/o CB)	Strong	No
251	*C8ORF46*	Olfactory Bulb, Telenceph (w/o hipp), Hipp	Strong	No
253	*PITX3*	Diencephalon, Midbrain, Hindbrain (w/o CB)	Strong	No
264	*NR2E1*	Olfactory Bulb, Telenceph (w/o hipp), Hipp	Strong	Yes; see Figure 5 and Table 4
265	*PCP2*	Eyes, Diencephalon, CB	Strong	Yes; see Figure 7 and Table 4
266	*S100B*	Midbrain, Hindbrain (w/o CB), CB	Strong	No
267	*UGT8*	Diencephalon, Midbrain, Hindbrain (w/o CB)	Strong	No
304	*OLIG1*	Telenceph (w/o hipp), Diencephalon, Midbrain	Strong	No
N/AP	hs671	Eyes, Telenceph (w/o hipp), Hipp	Strong	No
N/AP	hs1218	Telenceph (w/o hipp), Diencephalon, Midbrain	Strong	No
N/AP	*Hspa1a*[a]	Telenceph (w/o hipp), Hipp, Diencephalon	Strong	No
N/AP	CAGGS	Telenceph (w/o hipp), Hipp, Diencephalon	Strong	No
N/AP	(none)	Telenceph (w/o hipp), Diencephalon, Hindbrain (w/o CB)	Strong	No

Two to three key regions of interest were chosen for each strain and RNA prepared from N2 male mice. RT-PCR bands were scored as either: strong, weak, or very weak. MaxiPromoters are described first, followed by MiniPromoters below the line. CB, cerebellum; Hipp, hippocampus; N/AP, not applicable; Ple, Pleiades promoter; Telenceph, telencephalon; w/o, without.

[a] Synonym Hsp68.

This was presumably due to the influence of the genomic *Hprt* locus, despite the presence of insulators flanking the MiniPromoter inserts (Figure 1C). Using this RT-PCR data, a subset of strains was chosen for further breeding and tdTomato histological analysis. Two of the 10 MaxiPromoter strains were chosen, one strong and one weak expresser (Figure 2 and Figure 3). Four of the 17 MiniPromoter strains were chosen, and tested both as the inducible tm#a and constitutive tm#b alleles (Figures 4–7).

Ple272 CLDN5 MaxiPromoter expressed in the endothelial cells of the blood-retina and blood-brain barrier

Claudin 5 (CLDN5) is an integral membrane protein and component of tight junctions (Nitta *et al.* 2003). Tight junctions develop between endothelial cells of the blood vessels in the central nervous system, and play a key role in establishing the blood-brain barrier. Several diseases are associated with *CLDN5*, including velocardiofacial syndrome (Sirotkin *et al.* 1997) and gray platelet syndrome (Nurden *et al.* 2008). *CLDN5* was chosen for its expression in the endothelial cells of the blood-retina and blood-brain barrier.

In this inducible strain, the *CLDN5* MaxiPromoter expressed as expected for the endogenous gene in all tissues examined (Table 4). This included in the target blood vessels of the retina and brain (Figure 2). Expression was lower in female mice, as expected due to X-chromosome inactivation. Colabeling with anti-CLDN5 confirmed that expression localized to the endothelial cells of the blood vessels of the retina and brain. Mice carrying this inducible allele, who were fed a no-tamoxifen control diet, unexpectedly showed lower but still detectable levels of icre activity, which importantly remained restricted to the blood vessels of the retina and brain. This iCre "leakiness" (tamoxifen-independent Cre activity) rendered the strain constitutive at a low level and inducible to a high level (Murray *et al.* 2012). Finally, positive expression was also observed in the spinal cord and heart (Table 4), which was expected as blood vessels in the spinal cord and cardiomyocytes are known to express *CLDN5* (Sanford *et al.* 2005; Paul *et al.* 2013).

Ple274 CRH MaxiPromoter expressed in multiple endogenous brain regions, but showed only partial cellular overlap

Corticotropin-releasing hormone (CRH) is a neuropeptide that orchestrates the neuroendocrine, autonomic, and behavioral stress responses (Bale and Vale 2004). To this end, CRH possesses a dual mode of action: it acts as a secretagogue controlling the activity of the hypothalamic-pituitary-adrenal axis, and as a neuromodulator at extra hypothalamic sites.

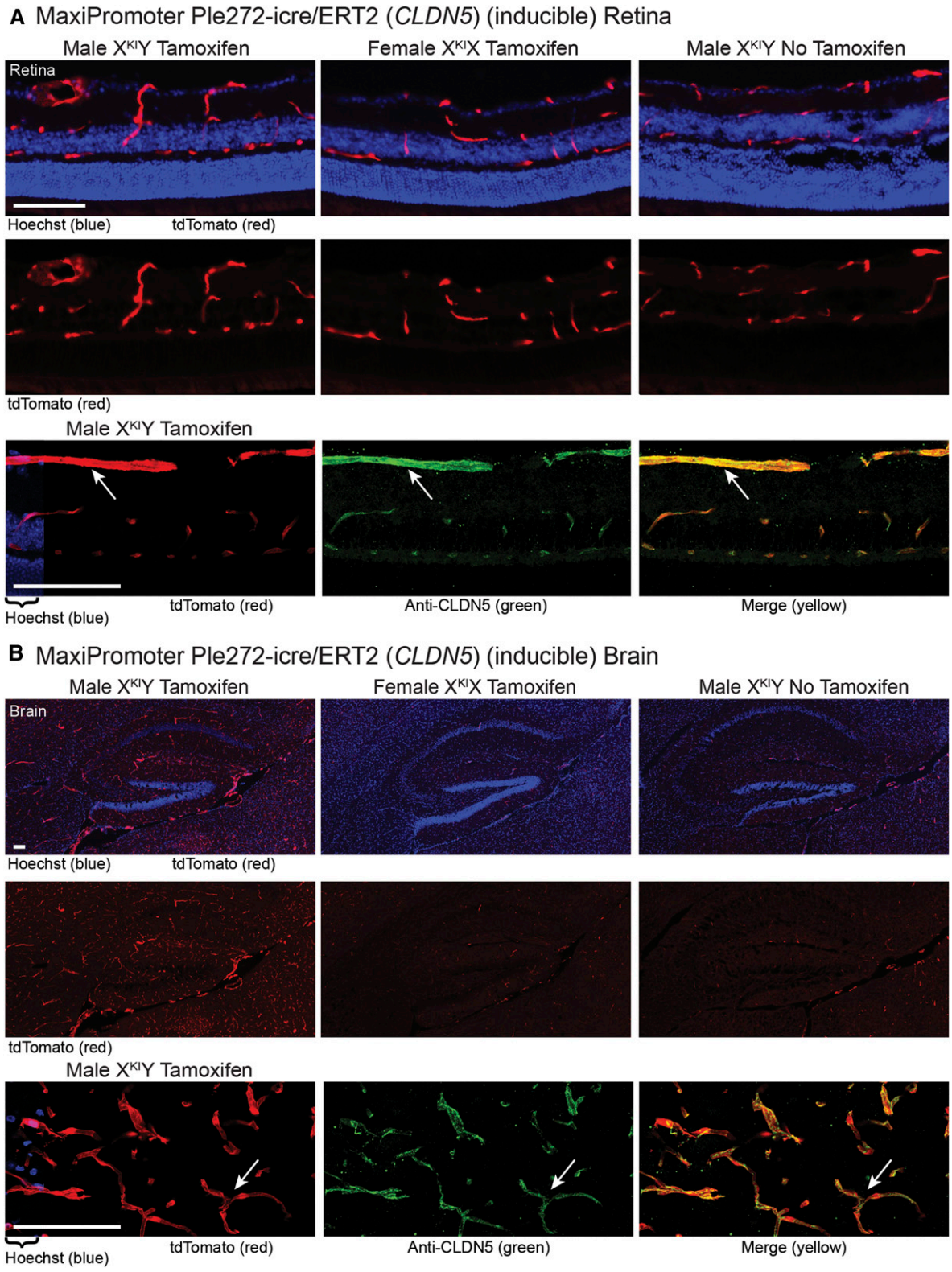

Figure 2 MaxiPromoter Ple272-icre/ERT2 (*CLDN5*) (inducible) expressed in the endothelial cells of the blood-retina and blood-brain barrier. Expression in the MaxiPromoter Ple272-icre/ERT2 strain was examined using tdTomato epifluorescence (red). Adult mice that carried both the icre/ERT2 and ROSA-Stop-tdTomato alleles were fed either tamoxifen or no tamoxifen. (A) Retina. First panel: tamoxifen fed male and female mice stained in the retinal blood vessels, with female staining slightly less as expected due to X-chromosome inactivation; no-tamoxifen male showed unexpected blood vessel staining due to icre "leakiness" (tamoxifen-independent cre activity). Hoechst nuclear stain (blue). Second panel: data shown without Hoechst. Third panel: tamoxifen fed male mouse costained with anti-CLDN5 antibody (green) demonstrated colabeling with tdTomato (merge, yellow) and thus endogenous-like expression in the

Several diseases are associated with *CRH*, including post-traumatic stress disorder (Hockings *et al.* 1993; Geracioti *et al.* 2008) and postpartum depression (McCoy *et al.* 2003; Meltzer-Brody *et al.* 2011). *CRH* was chosen particularly for its expression in the paraventricular hypothalamic nucleus (PvH), which is involved in neurohormonal mechanisms (Kovács 2013; Rigas *et al.* 2018).

In this inducible strain, the *CRH* MaxiPromoter showed a distribution of expressing neurons, which largely reflected the pattern of endogenous CRH (Merchenthaler *et al.* 1982; Keegan *et al.* 1994) (Table 4). Major *CRH* expression domains that contained tdTomato positive neurons included the piriform cortex (Pir), neocortex (Ctx), hippocampus, PvH, medial geniculate nucleus (MGM), Barrington nucleus, and inferior olive (Figure 3A). However, structures showed rather sparse labeling, which was lower in female mice as expected due to X-chromosome inactivation. Of note, some CRH-expressing brain regions such as the olfactory bulb, central amygdala, or bed nucleus of the stria terminals, showed only isolated tdTomato positive neurons. To investigate the coexpression of tdTomato with endogenous *CRH* expression at the cellular level we performed double ISH (Figure 3B). The double ISH revealed that, although the tdTomato positive neurons were generally located within the correct brain region, only a subset of neurons in a given structure coexpressed endogenous *Crh* mRNA. As expected, mice carrying this inducible allele, who were fed a no-tamoxifen control diet, did not show any tdTomato expression.

Ple155 PCP2 MiniPromoter expressed primarily in the retinal bipolar ON neurons

Purkinje cell protein (PCP2, aka. L7) may function as a modulator for G protein-mediated cell signaling (Zhang *et al.* 2002; Willard *et al.* 2006). PCP2 is involved in the maturation of cerebellar Purkinje cell neurons in the brain, but is also well recognized for its specificity to bipolar ON cell neurons of the retina in the eye (Vandaele *et al.* 1991). It was chosen for its expression in both these cell types, with the long-term goal of separating these expressions. We have previously demonstrated that the single MiniPromoter Ple155 (*PCP2*, 1652 bp) showed restricted expression in both the Purkinje and bipolar cells in X-chromosome knock-in mice driving lacZ (de Leeuw *et al.* 2014), and in rAAV driving icre and EmGFP (de Leeuw *et al.* 2016).

In the inducible strain (tm347a), the *PCP2* MiniPromoter showed endogenous-like expression in the retina, but was unexpectedly nonspecific in the brain (Table 4). In the retina, this included expression primarily in bipolar cells, but with low levels of expression in the ganglion cell layer (GCL) and in amacrine cells (Figure 4A). Expression was lower in female mice, as expected due to X-chromosome inactivation. Colabeling with anti-PCP2 confirmed that expression was localized primarily to the bipolar ON cells of the retina. Mice carrying this inducible allele, who were fed a no-tamoxifen control diet, were mainly negative, with only a few cells expressing.

In the constitutive strain (tm347b), the *PCP2* MiniPromoter was not specific, expressed throughout the retina and cornea, and remained nonspecific in the brain (Table 4). In the retina, expression was primarily in the inner nuclear layer (INL, bipolar and amacrine cells), and in the GCL and the Müller glia. In the cornea, expression was observed in all three layers of the cornea (epithelial, stromal, and endothelial) (Figure 4B). Expression was lower in female mice, as expected due to X-chromosome inactivation.

Ple265 PCP2, a smaller MiniPromoter, expressed primarily in the retinal bipolar ON neurons

To test if a smaller promoter could drive specific expression in only the bipolar ON neuronal cells of the retina, we designed Ple265 (*PCP2*, 986 bp), which is a 60% cut down of Ple155. Based on the bioinformatic design, Ple265 was expected to capture the bipolar expression pattern of the eye, but to eliminate brain expression. However, our results show that smaller Ple265 *PCP2* promoter maintained the same expression pattern as the larger Ple155 (*PCP2*).

In the inducible strain (tm348a), the *PCP2* MiniPromoter showed endogenous-like expression in the retina, but was unexpectedly positive and nonspecific in the brain (Table 4). In the retina, expression was primarily in the bipolar cells, but with low levels in the GCL and amacrine cells (Figure 5A). Colabeling with anti-PCP2 confirmed that retinal expression was localized primarily to the bipolar ON cells. Mice carrying this inducible allele, who were fed a no-tamoxifen control diet, were mainly negative, with only a few cells expressing.

In the constitutive strain (tm348b), the *PCP2* MiniPromoter was not specific and expressed throughout the retina and cornea, and was nonspecific in the brain (Figure 5B and Table 4). Expression was lower in female mice as expected due to X-chromosome inactivation.

Ple198 SLC6A4 MiniPromoter expressed in the retinal ganglion and amacrine cells

Solute carrier family 6 (neurotransmitter transporter, serotonin), member 4 (SLC6A4, aka SERT) is a transmembrane protein located on synaptic vesicles, and is involved in the transport of the neurotransmitter serotonin from synaptic spaces into presynaptic neurons (Lebrand *et al.* 1998). *SLC6A4* has been demonstrated to express primarily in the raphe nuclei of the brain. In the developing retina, ISH studies have demonstrated that *SLC6A4* is transcribed transiently

endothelial cells of the blood vessels (white arrow). (B) Brain. First panel: tamoxifen fed male and female mice stained in blood vessels of the brain (hippocampal region shown), with female staining less as expected due to X-chromosome inactivation; no-tamoxifen male showed some blood vessel staining due to icre leakiness. Hoechst nuclear stain (blue). Second panel: data shown without Hoechst. Third panel: tamoxifen fed male mouse costained with anti-CLDN5 antibody (green) demonstrated colabeling with tdTomato (merge, yellow) and thus endogenous-like expression in the endothelial cells of the blood vessels (white arrow). Bar, 100 μm.

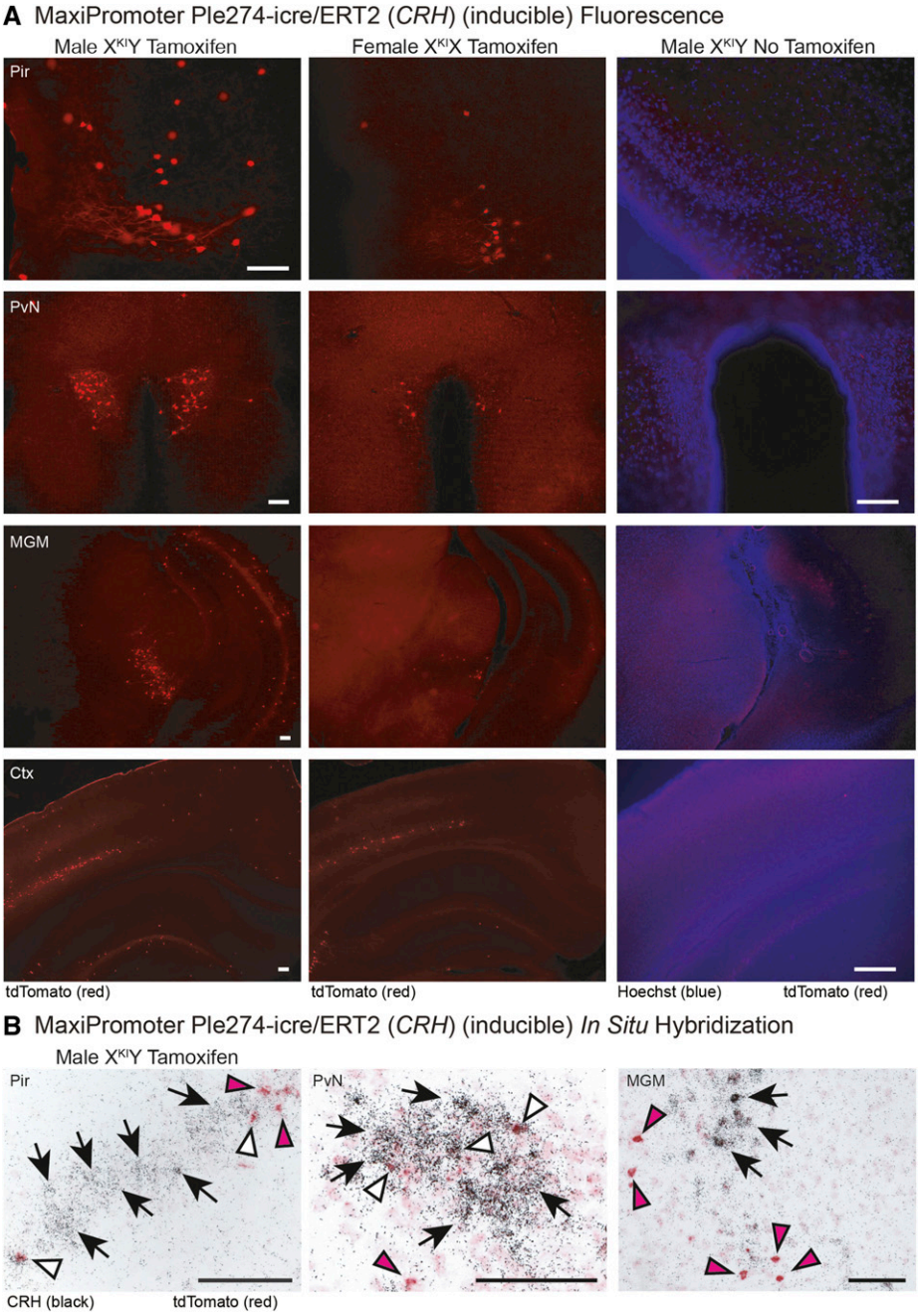

Figure 3 MaxiPromoter Ple274-icre/ERT2 (*CRH*) (inducible) expressed in the appropriate brain regions, but with partial cellular overlap. Expression in the MaxiPromoter Ple274-icre/ERT2 strain was examined using tdTomato epifluorescence (red). Adult mice that carried both the icre/ERT2 and ROSA-Stop-tdTomato alleles and were fed either tamoxifen or no tamoxifen [shown with Hoechst nuclear stain (blue)]. (A) Tamoxifen-fed male (first column) and female (second column) mice showed tdTomato positive neurons in brain regions representing major CRH expression domains including the piriform cortex (Pir), the paraventricular nucleus of the hypothalamus (PvN), the medial division of the medial geniculate (MGM), and the neocortex (Ctx). Female mice stained less as expected due to X-chromosome inactivation. Mice carrying this inducible allele, who were fed a no-tamoxifen control diet (third column), as expected did not show any tdTomato expression. (B) Tamoxifen fed male mouse was assessed for coexpression by double *in situ* hybridization. Depicted are bright field photomicrographs of coronal brain sections. Black arrows indicate cells expressing only *Crh* mRNA (silver grains). Red arrowheads indicate cells only expressing tdTomato mRNA (red staining). White arrowheads indicate cells coexpressing *Crh* and tdTomato. Bar, 100 μm.

in retinal ganglion cells (Upton *et al.* 1999; García-Frigola and Herrera 2010). Furthermore, a *SLC6A4*-cre mouse strain showed recombination in retinal ganglion cells (Assali *et al.* 2017). Several diseases are associated with *SLC6A4*, including obsessive-compulsive disorder (Sinopoli *et al.* 2017), anxiety (Arias *et al.* 2012), and post-traumatic stress disorder, as well as depression-susceptibility in people experiencing emotional trauma (Kuzelova *et al.* 2010). *SLC6A4* was originally chosen for the raphe nuclei, and we have previously demonstrated MiniPromoter Ple198 (*SLC6A4*, 2826 bp) showed, an expected restricted expression during development in the thalamus with rAAV driving icre (de Leeuw *et al.* 2016).

In the inducible strain (tm351a), the *SLC6A4* MiniPromoter expressed specifically in the retina and cornea, but nonspecifically in the brain, and thus did not capture the expected raphe expression (Table 4). In the retina, this included expression in widely spaced cells in the GCL, and in the cornea in the stromal cell layer (Figure 6A). Overall, expression was lower in female mice, as expected due to X-chromosome inactivation. Colabeling with anti-POU domain, class 4, transcription factor 1 (POU4F1, also known as BRN3A) confirmed expression in retinal ganglion cells in the GCL, and labeling with anti-glutamate decarboxylase 65/67 (GAD65/67) confirmed expression in GABAergic amacrine cells in the INL. However, anti-Calretinin and anti-tyrosine hydroxylase

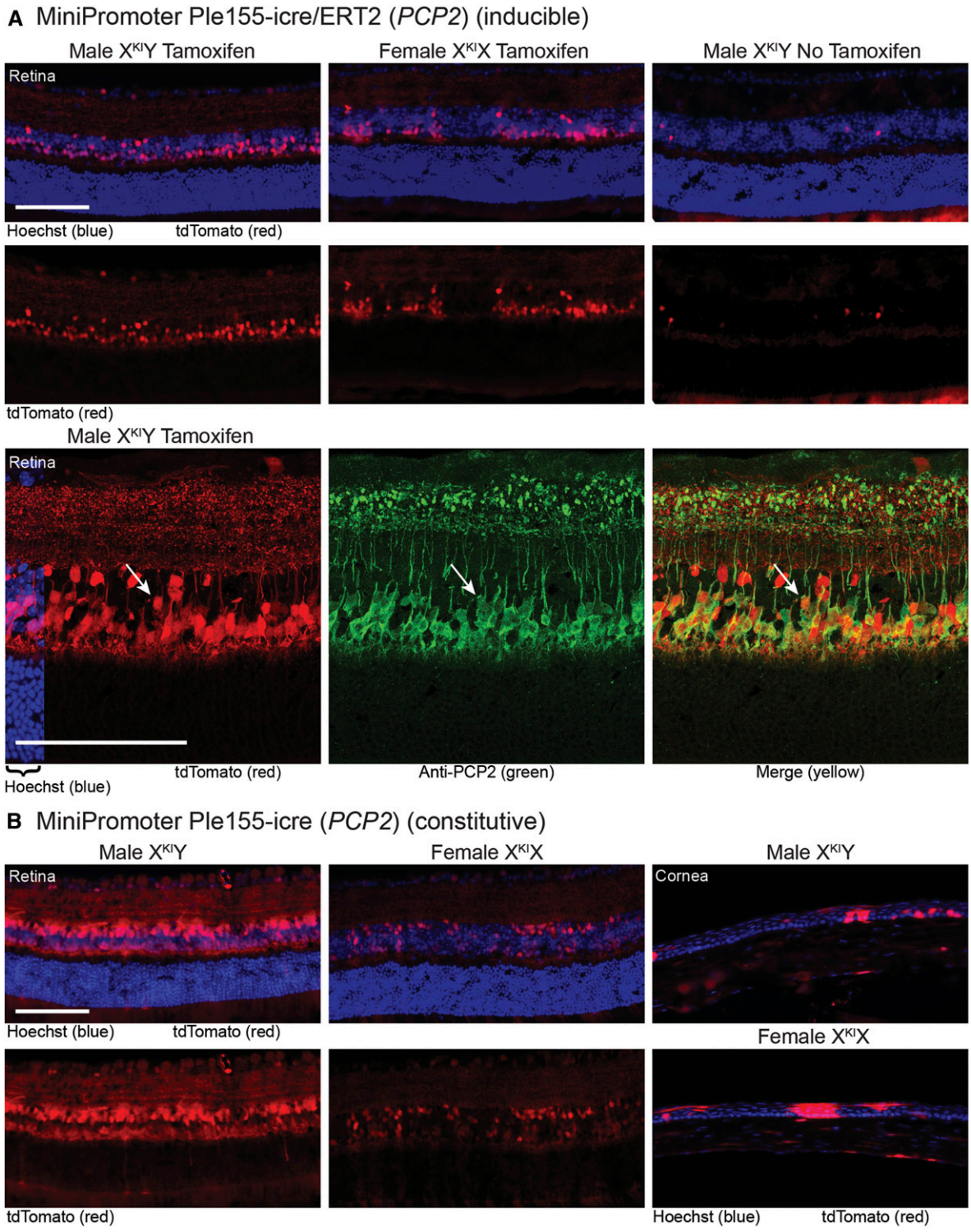

Figure 4 MiniPromoter Ple155-icre/f3/ERT2/f3 (*PCP2*) (inducible) expressed in the bipolar ON cells of the retina. Expression in the MiniPromoter Ple155-icre/f3/ERT2/f3 strain was examined both as an (A) inducible allele, and (B) constitutive allele using tdTomato epifluorescence (red). (A) Adult mice that carried both the inducible icre/f3/ERT2/f3 and ROSA-Stop-tdTomato alleles were fed either tamoxifen or no tamoxifen. First panel: tamoxifen fed male and female mice stained primarily in the bipolar cells of retina, with female staining slightly less as expected due to X-chromosome inactivation; no-tamoxifen male showed only occasional positive staining. Hoechst nuclear stain (blue). Second panel: data shown without Hoechst. Third panel: tamoxifen male mouse costained with anti-PCP2 antibody (green) demonstrating colabeling with tdTomato (merge, yellow), and thus endogenous-like expression in the bipolar ON cells of the retina (white arrow). (B) Adult mice that carried both the constitutive icre and ROSA-Stop-tdTomato alleles. First panel, columns 1 and 2: male and female mice stained throughout the retina (ganglion cell layer, inner nuclear layer, Müller glia), with female staining slightly less as expected due to X-chromosome inactivation. Second panel, columns 1 and 2: data shown without Hoechst. First and second panel, column 3: male and female mice stained throughout all three layers of the cornea (epithelial, stromal, and endothelial). Bar, 100 μm.

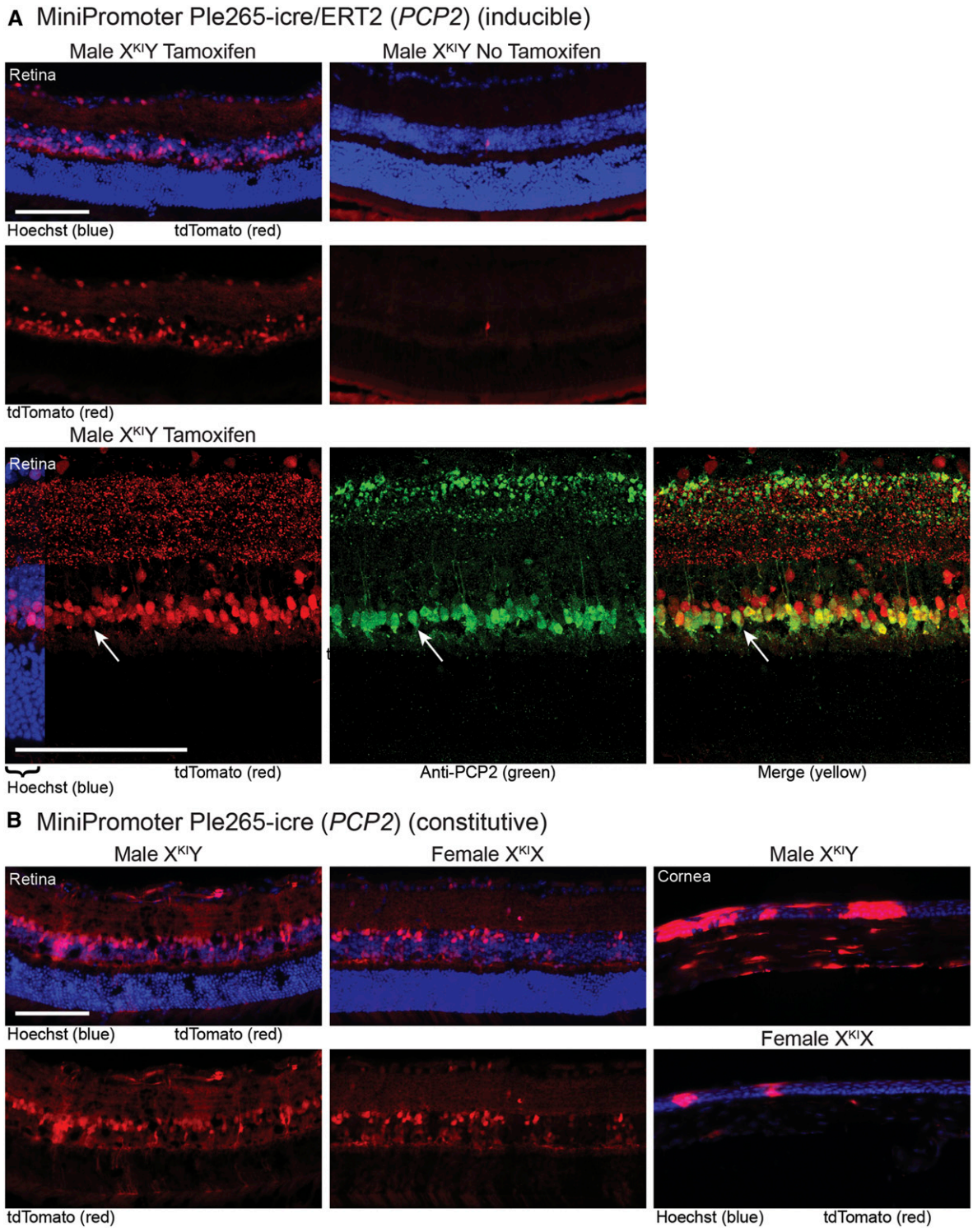

Figure 5 MiniPromoter Ple265-icre/f3/ERT2/f3 (*PCP2*) (inducible) expressed in the bipolar ON cells of the retina. Expression in the MiniPromoter Ple265-icre/f3/ERT2/f3 strain was examined both as an (A) inducible allele, and (B) constitutive allele using tdTomato epifluorescence (red). (A) Adult mice that carried both the inducible icre/f3/ERT2/f3 and ROSA-Stop-tdTomato alleles were fed either tamoxifen or no tamoxifen. First panel: tamoxifen fed male mice stained primarily in the bipolar cells of retina; no-tamoxifen male showed only occasional positive staining. Hoechst nuclear stain (blue). Second panel: data shown without Hoechst. Third panel: tamoxifen male mouse costained with anti-PCP2 antibody (green) demonstrating colabeling with tdTomato (merge, yellow), and thus endogenous-like expression in the bipolar ON cells of the retina (white arrow). (B) Adult mice that carried both the constitutive icre and ROSA-Stop-tdTomato alleles. First panel, columns 1 and 2: male and female mice stained throughout the retina (ganglion cell layer, inner nuclear layer, Müller glia), with female staining slightly less as expected due to X-chromosome inactivation. Second panel, columns 1 and 2: data shown without Hoechst. First and second panel, column 3: male and female mice stained throughout all three layers of the cornea (epithelial, stromal, and endothelial), with female staining less as expected due to X-chromosome inactivation. Bar, 100 μm.

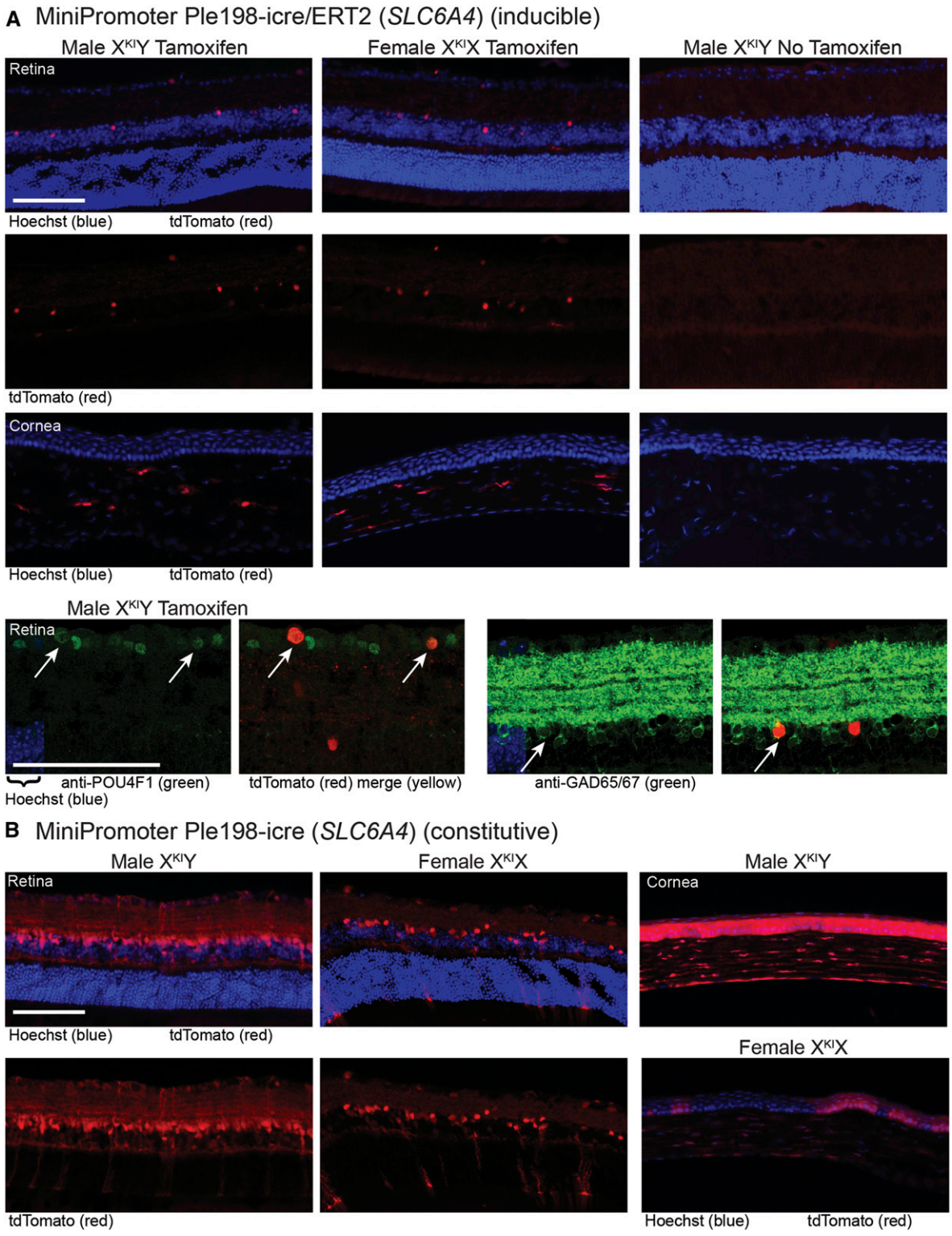

Figure 6 MiniPromoter Ple198-icre/f3/ERT2/f3 (*SLC6A4*) (inducible) expressed in retinal ganglion and amacrine cells. Expression in the MiniPromoter Ple198-icre/f3/ERT2/f3 strain was examined both as an (A) inducible allele, and (B) constitutive allele using tdTomato epifluorescence (red). (A) Adult mice that carried both the inducible icre/f3/ERT2/f3 and ROSA-Stop-tdTomato alleles were fed either tamoxifen or no tamoxifen. First panel: tamoxifen fed male and female mice stained in the ganglion cell layer and inner nuclear layer of the retina, with female overall staining slightly less as expected due to X-chromosome inactivation; no-tamoxifen male, as expected, did not show any tdTomato expression. Hoechst nuclear stain (blue). Second panel: data shown without Hoechst. Third panel: tamoxifen fed male and female mice stained in the stromal layer of the cornea, with female overall staining slightly less as expected due to X-chromosome inactivation; no-tamoxifen male, as expected, did not show any tdTomato expression. Fourth panel: tamoxifen male mouse costained with anti-POU4F1 (also known as BRN3A; green, columns 1 and 2) and anti-GAD65/67 (green, columns 3 and 4)

(TH) failed to label tdTomato-expressing cells (data not shown). As expected, mice carrying this inducible allele, who were fed a no-tamoxifen control diet, did not show any tdTomato expression.

In this constitutive strain (tm351b), the *SLC6A4* MiniPromoter was not specific and expressed throughout multiple layers of the retina and cornea, and nonspecifically in the brain, again not capturing the raphe expression (Table 4). In the retina, this included expression primarily in the INL, but also in the GCL and Müller glia, and in the cornea, this included the epithelial, stromal, and endothelial cell layers (Figure 6B). Overall, expression was lower in female mice, as expected due to X-chromosome inactivation.

As Ple198 (*SLC6A4*) expression was detected in POU4F1 immunoreactive retinal ganglion cells, it could be that this MiniPromoter recapitulates the endogenous expression in this cell type, but not in a developmental context. Additionally, serotonin uptake has been described in GABAergic amacrine cells in the mammalian retina (Osborne and Beaton 1986; Wassle and Chun 1988; Menger and Wassle 2000), although it is currently unclear if this uptake is conducted by SLC6A4. As tdTomato expression was detected in GAD65/67 immunoreactive amacrine cells, Ple198 (*SLC6A4*) could be recapitulating the endogenous expression in these cells. However, serotonin accumulating amacrines have been found to colabel with calretinin in *Xenopus laevis* (Gábriel 2000) and 90% of serotonin accumulating cells have been found to colabel with TH in the mouse retina (Trakhtenberg *et al.* 2017), but antibodies to either of these markers failed to colabel with tdTomato in this strain. Therefore, we can conclude expression is in a subset of GABAergic amacrines, but were not able to demonstrate that these were serotonin accumulating.

Ple264 NR2E1 MiniPromoter expressed primarily in the retinal Müller glia cells

Nuclear receptor subfamily 2, group E, member 1 (NR2E1) is a transcriptional regulator that has been demonstrated to play a critical role in brain and eye development (Stenman *et al.* 2003; Miyawaki *et al.* 2004; Christie *et al.* 2006; Corso-Díaz and Simpson 2015). NR2E1 is important in regulation of the processes that underlie neurogenesis, spatial learning, anxiety-like behavior, and aggression (Young *et al.* 2002; Abrahams *et al.* 2005; O'Leary *et al.* 2018). In addition, NR2E1 has been implicated in schizophrenia, bipolar disorder, metastatic castration-resistant prostate cancer, and post-stroke neurogenesis (Abdolmaleky *et al.* 2018; Jia *et al.* 2018; Nampoothiri *et al.* 2018). *NR2E1* was originally chosen for a neurogenic pattern in the brain and for the Müller glia of the retina (Miyawaki *et al.* 2004; Schmouth *et al.* 2012a; Corso-Díaz and Simpson 2015). We have previously demonstrated MiniPromoter Ple264 (*NR2E1*, 3026 bp) shows restricted expression in the Müller glia of the retina in rAAV (de Leeuw *et al.* 2016). Also, based on that work, we did not expect to capture the endogenous brain expression of *NR2E1* with this MiniPromoter.

In the inducible strain (tm346a), the *NR2E1* MiniPromoter expressed as expected in the retina and the brain (nonspecifically) (Table 4). In the retina, this included endogenous-like expression mainly in the Müller glia (Figure 7A). Expression was lower in female mice as expected due to X-chromosome inactivation. Colabeling with anti-Sox9 confirmed the expression was localized primarily to the Müller glia. As expected, mice carrying this inducible allele, who were fed a no-tamoxifen control diet, did not show any tdTomato expression.

In the constitutive strain (tm346b), the *NR2E1* MiniPromoter was not specific and expressed in an additional cell type in the retina, in the cornea, and as expected in the brain (nonspecifically) (Table 4). In the retina, this included expression in both amacrine and Müller glia, and in the cornea in the stromal and endothelial cell layers (Figure 7B). Expression was lower in female mice as expected due to X-chromosome inactivation.

Discussion

The first problem this work addressed was the need for more cre recombinase expressing transgenic mouse strains. We have substantially added to the cre-driver collection by developing 27 strains for cre expression in the brain and eye. These strains include 10 MaxiPromoters driving icre/ERT2, 14 MiniPromoters driving icre/f3/ERT2/f3 (from which 14 more constitutive alleles can be derived), and three controls driving icre/f3/ERT2/f3 (from which three more constitutive alleles can be derived). All strains were characterized by RT-PCR, and two MaxiPromoter and four MiniPromoter strains were also chosen for detailed characterization. Since both the inducible and constitutive alleles were characterized for the MiniPromoter strains, a total of 10 new cre alleles were characterized by crossing to cre-reporter mice followed by extensive histology.

We found the HuGX methodology, which docks constructs on the X Chromosome at the same site just 5′ of the *Hprt* gene (Schmouth *et al.* 2012b, 2013), to be rapid. MaxiPromoters (BACs) retrofitting with the homology arms (3 months) is substantially more challenging than MiniPromoters (plasmids) cloning (2 weeks), but from construct to germline is possible in 20 weeks. In both cases, the failure rate is low (9% (1/11) for MaxiPromoters, and 5% (1/19) for

demonstrating colabeling with tdTomato (merge, yellow), and thus expression in the retinal ganglion and GABAergic amacrine cells of the retina (white arrows). (B) Adult mice that carried both the constitutive icre and ROSA-Stop-tdTomato alleles. First panel, columns 1 and 2: male and female mice stained throughout the retina (ganglion cell layer, inner nuclear layer, Müller glia), with female staining slightly less as expected due to X-chromosome inactivation. Second panel, columns 1 and 2: data shown without Hoechst. First and second panel, column 3: male and female mice stained throughout all three layers of the cornea (epithelial, stromal, and endothelial), with female staining less as expected due to X-chromosome inactivation. Bar, 100 μm.

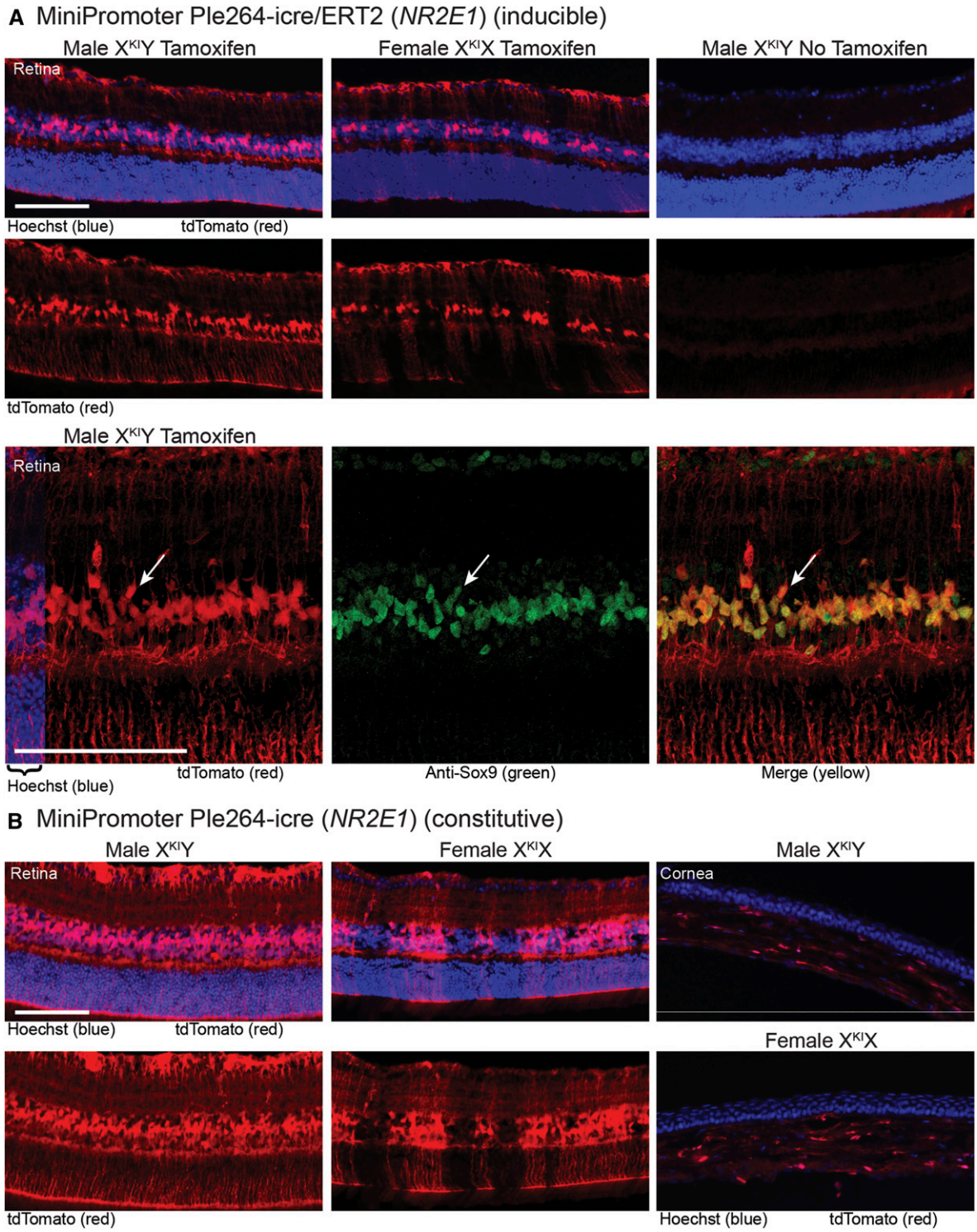

Figure 7 MiniPromoter Ple264-icre/f3/ERT2/f3 (*NR2E1*) (inducible) expressed in the Müller glia cells of the retina. Expression in the MiniPromoter Ple264-icre/f3/ERT2/f3 strain was examined both as an (A) inducible allele, and (B) constitutive allele using tdTomato epifluorescence (red). (A) Adult mice that carried both the inducible icre/f3/ERT2/f3 and ROSA-Stop-tdTomato alleles were fed either tamoxifen or no tamoxifen. First panel: tamoxifen fed male and female mice stained in the Müller glia of the retina, with female staining less as expected due to X-chromosome inactivation; no-tamoxifen male, as expected, did not show any tdTomato expression. Hoechst nuclear stain (blue). Second panel: data shown without Hoechst. Third panel: tamoxifen male mouse costained with anti-SOX9 (green) demonstrating colabeling with tdTomato (merge, yellow), and thus endogenous-like expression in the Müller glia cells of the retina (white arrow). (B) Adult mice that carried both the constitutive icre and ROSA-Stop-tdTomato alleles. First panel, columns 1 and 2: male and female mice stained in the amacrine cells and Müller glia of the retina, with female staining less as expected due to X-chromosome inactivation. Second panel, columns 1 and 2: data shown without Hoechst. First and second panel, column 3: male and female mice stained in the stromal and endothelial cell layers of the cornea, with female overall staining slightly less as expected due to X-chromosome inactivation. Bar, 100 μm.

Table 4 Summary of cre-reporter expression pattern for 10 strains

Ple	Gene	Allele	Retina	Cornea	Brain	Spinal cord	Heart
272	*CLDN5*	tm332	Positive: endothelial cells	Negative	Positive: endothelial cells	Positive	Positive
274	*CRH*	tm353	Negative	Negative	Positive: Ctx, MGM, Pir, PvH	Positive	Negative
155	*PCP2*	tm347a	Positive: primarily in bipolar cells, low level in amacrine and GCL	Negative	Positive: low level nonspecific[a] in the CB, Ctx, Hth, Thal	Negative	Negative
155	*PCP2*	tm347b	Positive: primarily in INL, low level in GCL and Müller glia	Positive: subset of endothelial, epithelial, stroma	Positive: high level nonspecific in the CB, Ctx, Hipp, Hth, OB, Stri, Thal	Negative	Positive
265	*PCP2*	tm348a	Positive: primarily in bipolar cells, low level in amacrine and GCL	Negative	Positive: low level nonspecific in the BS, Ctx, OB	Negative	Negative
265	*PCP2*	tm348b	Positive: primarily in INL, low level in GCL and Müller glia	Positive: subset of endothelial, epithelial, stroma	Positive: high level nonspecific in the CB, Ctx, Hipp, Hth, OB, Stri, Thal	Negative	Positive
198	*SLC6A4*	tm351a	Positive: widely spaced in the GCL and INL	Positive: stroma	Positive: low level nonspecific in the blood vessels	Positive	Positive
198	*SLC6A4*	tm351b	Positive: primarily in INL, low level in GCL and Müller glia	Positive: endothelial, epithelial, stroma	Positive: high level nonspecific in the blood vessels, Ctx, Hipp, Hth, OB, Stri, Thal	Positive	Positive
264	*NR2E1*	tm346a	Positive: primarily in Müller glia	Negative	Positive: low level nonspecific in the blood vessels, Ctx, Hipp, Hth, OB, Stri, Thal	Positive	Positive
264	*NR2E1*	tm346b	Positive: primarily in Müller glia, low levels in the INL	Positive: endothelial, stroma	Positive: high level nonspecific in the blood vessels, Ctx, Hipp, Hth, OB, Stri, Thal	Positive	Positive

tm#a (conditional) strains were crossed to a tdTomato cre reporter strain and expression induced in adult mice with tamoxifen. Tm#b (constitutive) strains were first generated by crossing tm#a strains to a flp germline-deleter strain to remove the ERT2 portion of the allele, and then the resulting tm#b was crossed to a tdTomato cre reporter strain. For both tm#a and tm#b, tdTomato expression was visualized from adult mouse tissue by epifluorescence. MaxiPromoters are described first, followed by MiniPromoters below the line. CB, cerebellum; Ctx, cortex; GCL, ganglion cell layer; Hth, hypothalamus; Hipp, hippocampus; INL, inner nuclear layer; MGM, medial geniculate; OB, olfactory bulb; Pir, piriform cortex; Ple, Pleiades promoter; PvN, paraventricular nucleus; Stri, striatum; Thal, thalamus.
[a] Neuronal and glial brain expression.

MiniPromoters), and occurred when, despite four or more correctly targeted ESC clones, all the chimeras failed to pass the targeted allele through the germline. Thus, this is a viable, rapid, methodology to make cre-driver strains.

The X-chromosome location of cre, resulting from the HuGX methodology, presents both a challenge and an opportunity. The challenge is related to fact that there are published examples where the sex of the parent carrying cre has been shown to broaden undesirably the deletion phenotype, secondary to expression in either the maternal and/or paternal germline (Hayashi *et al.* 2003; Kobayashi and Hensch 2013). With the *Hprt* knock-in strategy, when hemizygous males are desired for study, the cre allele must be brought through the maternal parent, without the option of shifting to the paternal if problems arise. However, using cell-specific promoters to drive cre, as in this study, should reduce or eliminate this challenge. The unique opportunity is that when the cre is brought through either the maternal or paternal parent, X-chromosome inactivation mosaic heterozygous females are obtained; mosaicism can be a useful analytical tool, as exemplified by this study of expression and others (Sakata *et al.* 2016; Renthal *et al.* 2018).

The most impressive endogenous-like expression for the MaxiPromoters was the *CLDN5* inducible strain, which showed reproducible strong expression in the blood vessel endothelial cells of the brain, eye, and spinal cord as expected (Nitta *et al.* 2003; Sanford *et al.* 2005; Paul *et al.* 2013). This strain also showed some iCre leakiness, but even this expression remained restricted to the blood vessels. Cre protein leakiness is a known concern associated with tamoxifen inducible alleles (Murray *et al.* 2012), and may be due to incomplete cre sequestering when a large amount of cre protein is produced. We conclude the BAC employed in this work contained all the necessary regulatory regions for endogenous expression of this gene, which is further supported by the successful MiniPromoters we have previously developed from this gene (Portales-Casamar *et al.* 2010; de Leeuw *et al.* 2014, 2016). This strain may be of particular interest as expression of proteins to modify, or temporarily open, the blood-brain barrier is of great interest for therapeutic accessibility to the brain. This cre-driver strain could be used to target the CLDN5-positive endothelial cells by both experiments employing breeding to a conditional allele, or by intravenous delivery of a cre-dependent virus.

The most impressive endogenous-like expression among the MiniPromoters was the *NR2E1* inducible strain, which showed reproducible strong expression in the Müller glia of the retina (Miyawaki *et al.* 2004; Schmouth *et al.* 2012a; Corso-Díaz and Simpson 2015). Based on previous studies in rAAV (de Leeuw *et al.* 2016), the MiniPromoter worked as expected, containing all the necessary regulatory regions for expression in Müller glia. Also, as predicted by the rAAV

studies, we observed a low level expression throughout the brain and not the endogenous neurogenic brain expression expected for this gene. This strain may be of particular use in that Müller glia are an important target in retinal therapy, since they provide essential components to the neurons of the retina and thus may be able to widely deliver a neuroprotective therapeutic (Ueki *et al.* 2015). This cre-driver strain could be used to target the Müller glia by both experiments employing breeding where the conditional allele expression is itself restricted, or by direct-eye delivery of a cre-dependent virus.

We were delighted with the functionality of the new inducible-first, constitutive-ready allele (icre/f_3/ERT2/f_3). With this allele, one targeted ESC line having gone germline allows the generation of two cre-driver strains. The initial strain carries a tamoxifen inducible conditional ice/ERT2 allele, and the second, after rearrangement by the Flp recombinase to remove ERT2, a constitutively active icre allele. We tested this allele by generating four pairs of MiniPromoter strains—inducible and constitutive—and showed the allele functioned as expected with no deleterious effect of the amino acids added by the presence of the f3 sites. In our work, which focused exclusively on adult mice, the inducible allele was the most informative, and the constitutive allele showed substantially broader and stronger expression, as expected of a historical marker capturing both embryonic and adult expression.

The second problem this work addressed was to restrict expression further, even beyond that of the endogenous gene, to specific cell types in the brain and eye for spatial and temporal control of cre-dependent genes. As highlighted above, there were some very successful strains produced by the HuGX strategy, but we also want to discuss examples of the challenges. Based on our previous overall success using human BACs to delineate noncoding regulatory regions of human brain genes (Schmouth *et al.* 2013), we were surprised by the result with the *CRH* gene. The *CRH* MaxiPromoter showed expression in the target regions of the brain, but only a subset of neurons in a given structure coexpressed endogenous *Crh* mRNA. This observation, however, is in line with previous reports demonstrating a significant amount of ectopic and missing expression observed in different *Crh-cre* driver and reporter strains (Keegan *et al.* 1994). Due to the partial overlap in correct expression observed, we expect that the missing expression is likely due to some regulatory element(s) that have not been captured in the selected BAC, or from the human regulatory regions present in the BAC being nonfunctional in the mouse. This strain represents an example of how, even with large BACs, the HuGX method can fail to reproduce fully the endogenous expression. In contrast, other groups have used 3′ knock-in at the endogenous mouse locus to produce successful *Crh* cre-drivers (Taniguchi *et al.* 2011; Krashes *et al.* 2014).

For the MiniPromoter strategy to narrow expression, we generated three controls strains, two with ubiquitous promoters (Hspa1a and CAGGS) and one promoterless (none), which were all analyzed by RT-PCR for cre transcription (Table 3). Of these, the unexpected and concerning result was the strong and widespread transcription obtained when no promoter was cloned into our MiniPromoter expression cassette, especially given the presence of flanking insulators. This was particularly surprising in that we (Portales-Casamar *et al.* 2010; de Leeuw *et al.* 2014), and others (Farhadi *et al.* 2003; Palais *et al.* 2009; Samuel *et al.* 2009), have successfully used this location 5′ of the ubiquitous *Hprt* gene for restricted expression of small promoters before, even without insulators. We were therefore delighted to find that when a specific promoter was placed into the current expression cassette, restricted expression could be obtained (Figures 4–7, and Table 4). Thus, we suspect the addition of insulators was of little value in our experiments, and the neutrality of the *Hprt* genomic region may not be as complete as previously thought (Farhadi *et al.* 2003; Palais *et al.* 2009; Schmouth *et al.* 2013; de Leeuw *et al.* 2014).

Another example of lack of locus neutrality may be the *PCP2* (Ple155) inducible MiniPromoter strain, which drove strong and reproducible expression specifically in the bipolar ON cells of the retina, as expected (de Leeuw *et al.* 2016). However, based on our previous results, and those of others, with Ple155 (*PCP2*) driving icre expression in rAAV (de Leeuw *et al.* 2016; Chan *et al.* 2017), we expected the *PCP2* (Ple155) inducible MiniPromoter strain to also drive specific expression in the Purkinje cells of the cerebellum. What we observed instead was low-level expression throughout the brain. We expect that this finding may be due to the ubiquitous *Hprt* locus influencing the expression of the promoter to become ubiquitous in the brain. Regardless, this strain may be of particular interest in that bipolar ON cells are an important target in retinal therapy for stationary night blindness and melanoma associated retinopathy (Scalabrino *et al.* 2015; Zeitz *et al.* 2015; Martemyanov and Sampath 2017), and may have additional utility in optogenetic strategies (Macé *et al.* 2015). This cre-driver strain could be used to target the bipolar ON cells by both experiments employing breeding where the conditional allele expression is itself restricted, or by direct-eye delivery of a cre-dependent virus.

In this evolving field, what do we see as the best way forward for further expanding the cre-driver collection and for cell-type restricted strains? Certainly, CRISPR has now made knocking-in cre at any mouse gene at least as fast and easy as docking 5′ of *Hprt*. Methods such as synthesized guide RNAs, short homology sequences, purified Cas9 protein, and direct introduction into mouse zygotes, have already enabled researchers to develop new constitutive and inducible cre-driver mice (Feng *et al.* 2016; Hasegawa *et al.* 2016; Ackermann *et al.* 2017; Mohsen *et al.* 2017; Daigle *et al.* 2018). However, with this strategy, the possibility remains of generating a deleterious allele in the very gene whose normal expression is to be captured. In this regard, it is probably best to avoid knock-in at the ATG, which typically produces a null allele and heterozygous mouse, in favor of knock-in at the 3′ end of the gene, but even this may produce

a hypomorphic allele affecting gene expression. Nevertheless, these endogenous-locus strategies are powerful and may very accurately capture the full complexity of the mouse gene expression. Combining them with the new inducible-first constitutive-ready allele developed here would add even further improvement. Still, the locus 5′ of the *Hprt* remains a viable option for a variety of situations, including when mutation of the endogenous gene is undesirable, when a BAC is likely to contain all the necessary regulatory regions (Maxi-Promoter), when the purpose is to capture only a portion of the natural endogenous expression (MiniPromoter), and when a human (or any nonmouse) gene is being used and studied. Thus, even today, multiple strategies for the generation of cre-driver strains are warranted.

Acknowledgments

We thank Alice Y. Chou for her support of the bioinformatics team; Sara Munro for her support in BAC DNA preparations; Sonia F. Black, Tom W. Johnson, and Tess C. Lengyell for making the mice; Olga Kaspieva and Stéphanie Laprise for their support with mouse breeding; Lisa J. Borretta for setting up protocols for histology; Kaelan Wong for perfusing the mice; and the following project Scientific Advisory Board members for their advice: Terry R. Magnuson (University of North Carolina), Edna Einsiedel (University of Calgary), William W. Hauswirth (University of Florida), and Timothy O'Connor (University of British Columbia). This work was funded by: Genome British Columbia AGCP-CanEuCre-01 award to D.G., W.W.W., R.A.H., and E.M.S.; the EU 6th and 7th Framework Integrated Programs, EUCOMM and EUCOMMTOOLS, to A.F.S.; and the German Federal Ministry of Education and Research, within the framework of the e:Med research and funding concept (IntegraMent: grant FKZ 01ZX1314H) to J.M.D. Also, salary support was provided by the University of British Columbia Four Year Doctoral Fellowship and Graduate Student Initiatives, and the Canadian Institutes of Health Research Canadian Graduate Scholarships to J.W.H. DG, WWW, RAH, EMS, and the University of British Columbia hold or have filed for US patents on a subset of the MiniPromoters. The other authors declare that they have no competing interests.

Literature Cited

Abdolmaleky, H. M., A. C. Gower, C. K. Wong, J. W. Cox, X. Zhang *et al.*, 2018 Aberrant transcriptomes and DNA methylomes define pathways that drive pathogenesis and loss of brain laterality/asymmetry in schizophrenia and bipolar disorder. Am. J. Med. Genet. B. Neuropsychiatr. Genet. https://doi.org/10.1002/ajmg.b.32691

Abrahams, B. S., M. C. Kwok, E. Trinh, S. Budaghzadeh, S. M. Hossain *et al.*, 2005 Pathological aggression in "fierce" mice corrected by human nuclear receptor 2E1. J. Neurosci. 25: 6263–6270. https://doi.org/10.1523/JNEUROSCI.4757-04.2005

Ackermann, A. M., J. Zhang, A. Heller, A. Briker, and K. H. Kaestner, 2017 High-fidelity Glucagon-CreER mouse line generated by CRISPR-Cas9 assisted gene targeting. Mol. Metab. 6: 236–244. https://doi.org/10.1016/j.molmet.2017.01.003

Anastassiadis, K., J. Fu, C. Patsch, S. Hu, S. Weidlich *et al.*, 2009 Dre recombinase, like Cre, is a highly efficient site-specific recombinase in E. coli, mammalian cells and mice. Dis. Model. Mech. 2: 508–515. https://doi.org/10.1242/dmm.003087

Arias, B., M. Aguilera, J. Moya, P. A. Saiz, H. Villa *et al.*, 2012 The role of genetic variability in the SLC6A4, BDNF and GABRA6 genes in anxiety-related traits. Acta Psychiatr. Scand. 125: 194–202. https://doi.org/10.1111/j.1600-0447.2011.01764.x

Ariza-Cosano, A., A. Visel, L. A. Pennacchio, H. B. Fraser, J. L. Gomez-Skarmeta *et al.*, 2012 Differences in enhancer activity in mouse and zebrafish reporter assays are often associated with changes in gene expression. BMC Genomics 13: 713. https://doi.org/10.1186/1471-2164-13-713

Arner, E., C. O. Daub, K. Vitting-Seerup, R. Andersson, B. Lilje *et al.*, 2015 Transcribed enhancers lead waves of coordinated transcription in transitioning mammalian cells. Science 347: 1010–1014. https://doi.org/10.1126/science.1259418

Assali, A., C. Le Magueresse, M. Bennis, X. Nicol, P. Gaspar *et al.*, 2017 RIM1/2 in retinal ganglion cells are required for the refinement of ipsilateral axons and eye-specific segregation. Sci. Rep. 7: 3236. https://doi.org/10.1038/s41598-017-03361-0

Bale, T. L., and W. W. Vale, 2004 CRF and CRF receptors: role in stress responsivity and other behaviors. Annu. Rev. Pharmacol. Toxicol. 44: 525–557. https://doi.org/10.1146/annurev.pharmtox.44.101802.121410

Bradley, A., K. Anastassiadis, A. Ayadi, J. F. Battey, C. Bell *et al.*, 2012 The mammalian gene function resource: the international knockout mouse consortium. Mamm. Genome 23: 580–586. https://doi.org/10.1007/s00335-012-9422-2

Bronson, S. K., E. G. Plaehn, K. D. Kluckman, J. R. Hagaman, N. Maeda *et al.*, 1996 Single-copy transgenic mice with chosen-site integration. Proc. Natl. Acad. Sci. USA 93: 9067–9072. https://doi.org/10.1073/pnas.93.17.9067

Chan, K. Y., M. J. Jang, B. B. Yoo, A. Greenbaum, N. Ravi *et al.*, 2017 Engineered AAVs for efficient noninvasive gene delivery to the central and peripheral nervous systems. Nat. Neurosci. 20: 1172–1179. https://doi.org/10.1038/nn.4593

Christie, B. R., A. M. Li, V. A. Redila, H. Booth, B. K. Y. Wong *et al.*, 2006 Deletion of the nuclear receptor *Nr2e1* impairs synaptic plasticity and dendritic structure in the mouse dentate gyrus. Neuroscience 137: 1031–1037. https://doi.org/10.1016/j.neuroscience.2005.08.091

Corso-Díaz, X., and E. M. Simpson, 2015 Nr2e1 regulates retinal lamination and the development of Müller glia, S-cones, and glycineric amacrine cells during retinogenesis. Mol. Brain 8: 37. https://doi.org/10.1186/s13041-015-0126-x

Daigle, T. L., L. Madisen, T. A. Hage, M. T. Valley, U. Knoblich *et al.*, 2018 A suite of transgenic driver and reporter mouse lines with enhanced brain-cell-type targeting and functionality. Cell 174: 465–480.e22. https://doi.org/10.1016/j.cell.2018.06.035

de Leeuw, C. N., F. M. Dyka, S. L. Boye, S. Laprise, M. Zhou *et al.*, 2014 Targeted CNS delivery using human MiniPromoters and demonstrated compatibility with adeno-associated viral vectors. Mol. Ther. Methods Clin. Dev. 1: 5. https://doi.org/10.1038/mtm.2013.5

de Leeuw, C. N., A. J. Korecki, G. E. Berry, J. W. Hickmott, S. L. Lam *et al.*, 2016 rAAV-compatible MiniPromoters for restricted expression in the brain and eye. Mol. Brain 9: 52. https://doi.org/10.1186/s13041-016-0232-4

Erdmann, G., G. Schutz, and S. Berger, 2007 Inducible gene inactivation in neurons of the adult mouse forebrain. BMC Neurosci. 8: 63. https://doi.org/10.1186/1471-2202-8-63

Farhadi, H. F., P. Lepage, R. Forghani, H. C. Friedman, W. Orfali *et al.*, 2003 A combinatorial network of evolutionarily con-

served myelin basic protein regulatory sequences confers distinct glial-specific phenotypes. J. Neurosci. 23: 10214–10223. https://doi.org/10.1523/JNEUROSCI.23-32-10214.2003

Feil, R., J. Wagner, D. Metzger, and P. Chambon, 1997 Regulation of Cre recombinase activity by mutated estrogen receptor ligand-binding domains. Biochem. Biophys. Res. Commun. 237: 752–757. https://doi.org/10.1006/bbrc.1997.7124

Feng, J., J. Jing, P. A. Sanchez-Lara, M. S. Bootwalla, J. Buckley *et al.*, 2016 Generation and characterization of tamoxifen-inducible Pax9-CreER knock-in mice using CrispR/Cas9. Genesis 54: 490–496. https://doi.org/10.1002/dvg.22956

Gábriel, R., 2000 Calretinin is present in serotonin- and gamma-aminobutyric acid-positive amacrine cell populations in the retina of Xenopus laevis. Neurosci. Lett. 285: 9–12. https://doi.org/10.1016/S0304-3940(00)01005-3

García-Frigola, C., and E. Herrera, 2010 Zic2 regulates the expression of Sert to modulate eye-specific refinement at the visual targets. EMBO J. 29: 3170–3183. https://doi.org/10.1038/emboj.2010.172

Geracioti, Jr., T. D., D. G. Baker, J. W. Kasckow, J. R. Strawn, J. Jeffrey Mulchahey *et al.*, 2008 Effects of trauma-related audiovisual stimulation on cerebrospinal fluid norepinephrine and corticotropin-releasing hormone concentrations in post-traumatic stress disorder. Psychoneuroendocrinology 33: 416–424. https://doi.org/10.1016/j.psyneuen.2007.12.012

Hasegawa, Y., Y. Hoshino, A. E. Ibrahim, K. Kato, Y. Daitoku *et al.*, 2016 Generation of CRISPR/Cas9-mediated bicistronic knock-in ins1-cre driver mice. Exp. Anim. 65: 319–327. https://doi.org/10.1538/expanim.16-0016

Hayashi, S., T. Tenzen, and A. P. McMahon, 2003 Maternal inheritance of Cre activity in a Sox2Cre deleter strain. Genesis 37: 51–53. https://doi.org/10.1002/gene.10225

Heaney, J. D., A. N. Rettew, and S. K. Bronson, 2004 Tissue-specific expression of a BAC transgene targeted to the Hprt locus in mouse embryonic stem cells. Genomics 83: 1072–1082. https://doi.org/10.1016/j.ygeno.2003.12.015

Hickmott, J. W., C. Y. Chen, D. J. Arenillas, A. J. Korecki, S. L. Lam *et al.*, 2016 PAX6 MiniPromoters drive restricted expression from rAAV in the adult mouse retina. Mol. Ther. Methods Clin. Dev. 3: 16051. https://doi.org/10.1038/mtm.2016.51

Hockings, G. I., J. E. Grice, W. K. Ward, M. M. Walters, G. R. Jensen *et al.*, 1993 Hypersensitivity of the hypothalamic-pituitary-adrenal axis to naloxone in post-traumatic stress disorder. Biol. Psychiatry 33: 585–593. https://doi.org/10.1016/0006-3223(93)90096-V

Hoess, R. H., A. Wierzbicki, and K. Abremski, 1986 The role of the loxP spacer region in P1 site-specific recombination. Nucleic Acids Res. 14: 2287–2300. https://doi.org/10.1093/nar/14.5.2287

Indra, A. K., X. Warot, J. Brocard, J. M. Bornert, J. H. Xiao *et al.*, 1999 Temporally-controlled site-specific mutagenesis in the basal layer of the epidermis: comparison of the recombinase activity of the tamoxifen-inducible Cre-ER(T) and Cre-ER(T2) recombinases. Nucleic Acids Res. 27: 4324–4327. https://doi.org/10.1093/nar/27.22.4324

Jia, L., D. Wu, Y. Wang, W. You, Z. Wang *et al.*, 2018 Orphan nuclear receptor TLX contributes to androgen insensitivity in castration-resistant prostate cancer via its repression of androgen receptor transcription. Oncogene 37: 3340–3355. https://doi.org/10.1038/s41388-018-0198-z

Kaloff, C., K. Anastassiadis, A. Ayadi, R. Baldock, M.-C. Birling *et al.*, 2017 Genome-wide conditional mouse knockout resources. Drug Discov. Today 20: 3–12.

Keegan, C. E., J. P. Herman, I. J. Karolyi, K. S. O'Shea, S. A. Camper *et al.*, 1994 Differential expression of corticotropin-releasing hormone in developing mouse embryos and adult brain. Endocrinology 134: 2547–2555. https://doi.org/10.1210/endo.134.6.8194481

Kobayashi, Y., and T. K. Hensch, 2013 Germline recombination by conditional gene targeting with Parvalbumin-Cre lines. Front. Neural Circuits 7: 168. https://doi.org/10.3389/fncir.2013.00168

Kovács, K. J., 2013 CRH: the link between hormonal-, metabolic- and behavioral responses to stress. J. Chem. Neuroanat. 54: 25–33. https://doi.org/10.1016/j.jchemneu.2013.05.003

Krashes, M. J., B. P. Shah, J. C. Madara, D. P. Olson, D. E. Strochlic *et al.*, 2014 An excitatory paraventricular nucleus to AgRP neuron circuit that drives hunger. Nature 507: 238–242. https://doi.org/10.1038/nature12956

Kuzelova, H., R. Ptacek, and M. Macek, 2010 The serotonin transporter gene (5-HTT) variant and psychiatric disorders: review of current literature. Neuroendocrinol. Lett. 31: 4–10.

Lebrand, C., O. Cases, R. Wehrlé, R. D. Blakely, R. H. Edwards *et al.*, 1998 Transient developmental expression of monoamine transporters in the rodent forebrain. J. Comp. Neurol. 401: 506–524. https://doi.org/10.1002/(SICI)1096-9861(19981130)401:4<506::AID-CNE5>3.0.CO;2-#

Lyznik, L. A., J. C. Mitchell, L. Hirayama, and T. K. Hodges, 1993 Activity of yeast FLP recombinase in maize and rice protoplasts. Nucleic Acids Res. 21: 969–975. https://doi.org/10.1093/nar/21.4.969

Macé, E., R. Caplette, O. Marre, A. Sengupta, A. Chaffiol *et al.*, 2015 Targeting channelrhodopsin-2 to ON-bipolar cells with vitreally administered AAV restores ON and OFF visual responses in blind mice. Mol. Ther. 23: 7–16. https://doi.org/10.1038/mt.2014.154

Madisen, L., T. A. Zwingman, S. M. Sunkin, S. W. Oh, H. A. Zariwala *et al.*, 2010 A robust and high-throughput Cre reporting and characterization system for the whole mouse brain. Nat. Neurosci. 13: 133–140. https://doi.org/10.1038/nn.2467

Martemyanov, K. A., and A. P. Sampath, 2017 The transduction cascade in retinal ON-bipolar cells: signal processing and disease. Annu. Rev. Vis. Sci. 3: 25–51. https://doi.org/10.1146/annurev-vision-102016-061338

McCoy, S. J., J. M. Beal, and G. H. Watson, 2003 Endocrine factors and postpartum depression. A selected review. J. Reprod. Med. 48: 402–408.

Meltzer-Brody, S., A. Stuebe, N. Dole, D. Savitz, D. Rubinow *et al.*, 2011 Elevated corticotropin releasing hormone (CRH) during pregnancy and risk of postpartum depression (PPD). J. Clin. Endocrinol. Metab. 96: E40–E47. https://doi.org/10.1210/jc.2010-0978

Menger, N., and H. Wassle, 2000 Morphological and physiological properties of the A17 amacrine cell of the rat retina. Vis. Neurosci. 17: 769–780. https://doi.org/10.1017/S0952523800175108

Merchenthaler, I., S. Vigh, P. Petrusz, and A. V. Schally, 1982 Immunocytochemical localization of corticotropin-releasing factor (CRF) in the rat brain. Am. J. Anat. 165: 385–396. https://doi.org/10.1002/aja.1001650404

Metzger, D., and R. Feil, 1999 Engineering the mouse genome by site-specific recombination. Curr. Opin. Biotechnol. 10: 470–476. https://doi.org/10.1016/S0958-1669(99)00012-9

Miyawaki, T., A. Uemura, M. Dezawa, R. T. Yu, C. Ide *et al.*, 2004 Tlx, an orphan nuclear receptor, regulates cell numbers and astrocyte development in the developing retina. J. Neurosci. 24: 8124–8134. https://doi.org/10.1523/JNEUROSCI.2235-04.2004

Mohsen, Z., H. Sim, D. Garcia-Galiano, X. Han, N. Bellefontaine *et al.*, 2017 Sexually dimorphic distribution of Prokr2 neurons revealed by the Prokr2-Cre mouse model. Brain Struct. Funct. 222: 4111–4129. https://doi.org/10.1007/s00429-017-1456-5

Murray, S. A., J. T. Eppig, D. Smedley, E. M. Simpson, and N. Rosenthal, 2012 Beyond knockouts: cre resources for conditional mutagenesis. Mamm. Genome 23: 587–599. https://doi.org/10.1007/s00335-012-9430-2

Muzumdar, M. D., B. Tasic, K. Miyamichi, L. Li, and L. Luo, 2007 A global double-fluorescent Cre reporter mouse. Genesis 45: 593–605. https://doi.org/10.1002/dvg.20335

Nampoothiri, S. S., S. M. Fayaz, and G. K. Rajanikant, 2018 A novel five-node feed-forward loop unravels miRNA-gene-TF regulatory relationships in ischemic stroke. Mol. Neurobiol. 55: 8251–8262. https://doi.org/10.1007/s12035-018-0963-6

Nitta, T., M. Hata, S. Gotoh, Y. Seo, H. Sasaki *et al.*, 2003 Size-selective loosening of the blood-brain barrier in claudin-5-deficient mice. J. Cell Biol. 161: 653–660. https://doi.org/10.1083/jcb.200302070

Nurden, A. T., P. Nurden, E. Bermejo, R. Combrié, D. W. McVicar *et al.*, 2008 Phenotypic heterogeneity in the Gray platelet syndrome extends to the expression of TREM family member, TLT-1. Thromb. Haemost. 100: 45–51. https://doi.org/10.1160/TH08-02-0067

O'Leary, J. D., O. F. O'Leary, J. F. Cryan, and Y. M. Nolan, 2018 Regulation of behaviour by the nuclear receptor TLX. Genes Brain Behav. 17: e12357. https://doi.org/10.1111/gbb.12357

Osborne, N. N., and D. W. Beaton, 1986 Direct histochemical localisation of 5,7-dihydroxytryptamine and the uptake of serotonin by a subpopulation of GABA neurones in the rabbit retina. Brain Res. 382: 158–162. https://doi.org/10.1016/0006-8993(86)90125-3

Palais, G., A. Nguyen Dinh Cat, H. Friedman, N. Panek-Huet, A. Millet *et al.*, 2009 Targeted transgenesis at the HPRT locus: an efficient strategy to achieve tightly controlled in vivo conditional expression with the tet system. Physiol. Genomics 37: 140–146. https://doi.org/10.1152/physiolgenomics.90328.2008

Paul, D., A. E. Cowan, S. Ge, and J. S. Pachter, 2013 Novel 3D analysis of Claudin-5 reveals significant endothelial heterogeneity among CNS microvessels. Microvasc. Res. 86: 1–10. https://doi.org/10.1016/j.mvr.2012.12.001

Peeters, S. B., A. J. Korecki, E. M. Simpson, and C. J. Brown, 2018 Human cis-acting elements regulating escape from X-chromosome inactivation function in mouse. Hum. Mol. Genet. 27: 1252–1262. https://doi.org/10.1093/hmg/ddy039

Portales-Casamar, E., D. J. Swanson, L. Liu, C. N. de Leeuw, K. G. Banks *et al.*, 2010 A regulatory toolbox of MiniPromoters to drive selective expression in the brain. Proc. Natl. Acad. Sci. USA 107: 16589–16594. https://doi.org/10.1073/pnas.1009158107

Raymond, C. S., and P. Soriano, 2007 High-efficiency FLP and PhiC31 site-specific recombination in mammalian cells. PLoS One 2: e162. https://doi.org/10.1371/journal.pone.0000162

Refojo, D., M. Schweizer, C. Kuehne, S. Ehrenberg, C. Thoeringer *et al.*, 2011 Glutamatergic and dopaminergic neurons mediate anxiogenic and anxiolytic effects of CRHR1. Science 333: 1903–1907. https://doi.org/10.1126/science.1202107

Renthal, W., L. D. Boxer, S. Hrvatin, E. Li, A. Silberfeld *et al.*, 2018 Characterization of human mosaic Rett syndrome brain tissue by single-nucleus RNA sequencing. Nat. Neurosci. 21: 1670–1679. https://doi.org/10.1038/s41593-018-0270-6

Rigas, A., D. Farmakis, G. Papingiotis, G. Bakosis, and J. Parissis, 2018 Hypothalamic dysfunction in heart failure: pathogenetic mechanisms and therapeutic implications. Heart Fail. Rev. 23: 55–61. https://doi.org/10.1007/s10741-017-9659-7

Rosen, B., J. Schick, and W. Wurst, 2015 Beyond knockouts: the International Knockout Mouse Consortium delivers modular and evolving tools for investigating mammalian genes. Mamm. Genome 26: 456–466. https://doi.org/10.1007/s00335-015-9598-3

Ruzankina, Y., C. Pinzon-Guzman, A. Asare, T. Ong, L. Pontano *et al.*, 2007 Deletion of the developmentally essential gene ATR in adult mice leads to age-related phenotypes and stem cell loss. Cell Stem Cell 1: 113–126. https://doi.org/10.1016/j.stem.2007.03.002

Sakata, K., K. Araki, H. Nakano, T. Nishina, S. Komazawa-Sakon *et al.*, 2016 Novel method to rescue a lethal phenotype through integration of target gene onto the X-chromosome. Sci. Rep. 6: 37200. https://doi.org/10.1038/srep37200

Sakurai, K., M. Shimoji, C. G. Tahimic, K. Aiba, E. Kawase *et al.*, 2010 Efficient integration of transgenes into a defined locus in human embryonic stem cells. Nucleic Acids Res. 38: e96. https://doi.org/10.1093/nar/gkp1234

Samuel, M. S., J. Munro, S. Bryson, S. Forrow, D. Stevenson *et al.*, 2009 Tissue selective expression of conditionally-regulated rock by gene targeting to a defined locus. Genesis 47: 440–446. https://doi.org/10.1002/dvg.20519

Sanford, J. L., J. D. Edwards, T. A. Mays, B. Gong, A. P. Merriam *et al.*, 2005 Claudin-5 localizes to the lateral membranes of cardiomyocytes and is altered in utrophin/dystrophin-deficient cardiomyopathic mice. J. Mol. Cell. Cardiol. 38: 323–332. https://doi.org/10.1016/j.yjmcc.2004.11.025

Scalabrino, M. L., S. L. Boye, K. M. Fransen, J. M. Noel, F. M. Dyka *et al.*, 2015 Intravitreal delivery of a novel AAV vector targets ON bipolar cells and restores visual function in a mouse model of complete congenital stationary night blindness. Hum. Mol. Genet. 24: 6229–6239. https://doi.org/10.1093/hmg/ddv341

Schlake, T., and J. Bode, 1994 Use of mutated FLP recognition target (FRT) sites for the exchange of expression cassettes at defined chromosomal loci. Biochemistry 33: 12746–12751. https://doi.org/10.1021/bi00209a003

Schmouth, J.-F., K. G. Banks, A. Mathelier, C. Y. Gregory-Evans, M. Castellarin *et al.*, 2012a Retina restored and brain abnormalities ameliorated by single-copy knock-in of human NR2E1 in null mice. Mol. Cell. Biol. 32: 1296–1311. https://doi.org/10.1128/MCB.06016-11

Schmouth, J. F., R. J. Bonaguro, X. Corso-Diaz, and E. M. Simpson, 2012b Modelling human regulatory variation in mouse: finding the function in genome-wide association studies and whole-genome sequencing. PLoS Genet. 8: e1002544.

Schmouth, J. F., M. Castellarin, S. Laprise, K. G. Banks, R. J. Bonaguro *et al.*, 2013 Non-coding-regulatory regions of human brain genes delineated by bacterial artificial chromosome knock-in mice. BMC Biol. 11: 106. https://doi.org/10.1186/1741-7007-11-106

Shimshek, D. R., J. Kim, M. R. Hubner, D. J. Spergel, F. Buchholz *et al.*, 2002 Codon-improved Cre recombinase (iCre) expression in the mouse. Genesis 32: 19–26. https://doi.org/10.1002/gene.10023

Simpson, E., A. J. Korecki, O. Fornes, T. J. McGill, J. L. Cueva-Vargas *et al.*, 2018 New MiniPromoter Ple345 (NEFL) drives strong and specific expression in retinal ganglion cells of mouse and primate retina. Hum. Gene Ther. .https://doi.org/10.1089/hum.2018.118

Sinopoli, V. M., C. L. Burton, S. Kronenberg, and P. D. Arnold, 2017 A review of the role of serotonin system genes in obsessive-compulsive disorder. Neurosci. Biobehav. Rev. 80: 372–381. https://doi.org/10.1016/j.neubiorev.2017.05.029

Sirotkin, H., B. Morrow, B. Saint-Jore, A. Puech, R. Das Gupta *et al.*, 1997 Identification, characterization, and precise mapping of a human gene encoding a novel membrane-spanning protein from the 22q11 region deleted in velo-cardio-facial syndrome. Genomics 42: 245–251. https://doi.org/10.1006/geno.1997.4734

Soriano, P., 1999 Generalized lacZ expression with the ROSA26 Cre reporter strain. Nat. Genet. 21: 70–71. https://doi.org/10.1038/5007

Stenman, J. M., B. Wang, and K. Campbell, 2003 Tlx controls proliferation and patterning of lateral telencephalic progenitor domains. J. Neurosci. 23: 10568–10576. https://doi.org/10.1523/JNEUROSCI.23-33-10568.2003

Taniguchi, H., M. He, P. Wu, S. Kim, R. Paik *et al.*, 2011 A resource of Cre driver lines for genetic targeting of GABAergic

neurons in cerebral cortex. Neuron 71: 995–1013. https://doi.org/10.1016/j.neuron.2011.07.026

Trakhtenberg, E. F., W. Pita-Thomas, S. G. Fernandez, K. H. Patel, P. Venugopalan *et al.*, 2017 Serotonin receptor 2C regulates neurite growth and is necessary for normal retinal processing of visual information. Dev. Neurobiol. 77: 419–437. https://doi.org/10.1002/dneu.22391

Ueki, Y., M. S. Wilken, K. E. Cox, L. Chipman, N. Jorstad *et al.*, 2015 Transgenic expression of the proneural transcription factor Ascl1 in Muller glia stimulates retinal regeneration in young mice. Proc. Natl. Acad. Sci. USA 112: 13717–13722. https://doi.org/10.1073/pnas.1510595112

Upton, A. L., N. Salichon, C. Lebrand, A. Ravary, R. Blakely *et al.*, 1999 Excess of serotonin (5-HT) alters the segregation of ispilateral and contralateral retinal projections in monoamine oxidase A knock-out mice: possible role of 5-HT uptake in retinal ganglion cells during development. J. Neurosci. 19: 7007–7024. https://doi.org/10.1523/JNEUROSCI.19-16-07007.1999

Vandaele, S., D. T. Nordquist, R. M. Feddersen, I. Tretjakoff, A. C. Peterson *et al.*, 1991 Purkinje cell protein-2 regulatory regions and transgene expression in cerebellar compartments. Genes Dev. 5: 1136–1148. https://doi.org/10.1101/gad.5.7.1136

Visel, A., S. Minovitsky, I. Dubchak, and L. A. Pennacchio, 2007 VISTA Enhancer Browser–a database of tissue-specific human enhancers. Nucleic Acids Res. 35: D88–D92. https://doi.org/10.1093/nar/gkl822

Wassle, H., and M. H. Chun, 1988 Dopaminergic and indoleamine-accumulating amacrine cells express GABA-like immunoreactivity in the cat retina. J. Neurosci. 8: 3383–3394. https://doi.org/10.1523/JNEUROSCI.08-09-03383.1988

Willard, F. S., C. R. McCudden, and D. P. Siderovski, 2006 G-protein alpha subunit interaction and guanine nucleotide dissociation inhibitor activity of the dual GoLoco motif protein PCP-2 (Purkinje cell protein-2). Cell. Signal. 18: 1226–1234. https://doi.org/10.1016/j.cellsig.2005.10.003

Yang, G. S., K. G. Banks, R. J. Bonaguro, G. Wilson, L. Dreolini *et al.*, 2009 Next generation tools for high-throughput promoter and expression analysis employing single-copy knock-ins at the *Hprt1* locus. Genomics 93: 196–204. https://doi.org/10.1016/j.ygeno.2008.09.014

Young, K. A., M. L. Berry, C. L. Mahaffey, J. R. Saionz, N. L. Hawes *et al.*, 2002 Fierce: a new mouse deletion of *Nr2e1*; violent behaviour and ocular abnormalities are background-dependent. Behav. Brain Res. 132: 145–158. https://doi.org/10.1016/S0166-4328(01)00413-2

Yu, D., H. M. Ellis, E. C. Lee, N. A. Jenkins, N. G. Copeland *et al.*, 2000 An efficient recombination system for chromosome engineering in Escherichia coli. Proc. Natl. Acad. Sci. USA 97: 5978–5983. https://doi.org/10.1073/pnas.100127597

Zanta-Boussif, M. A., S. Charrier, A. Brice-Ouzet, S. Martin, P. Opolon *et al.*, 2009 Validation of a mutated PRE sequence allowing high and sustained transgene expression while abrogating WHV-X protein synthesis: application to the gene therapy of WAS. Gene Ther. 16: 605–619. https://doi.org/10.1038/gt.2009.3

Zeitz, C., A. G. Robson, and I. Audo, 2015 Congenital stationary night blindness: an analysis and update of genotype-phenotype correlations and pathogenic mechanisms. Prog. Retin. Eye Res. 45: 58–110. https://doi.org/10.1016/j.preteyeres.2014.09.001

Zhang, X., H. Zhang, and J. Oberdick, 2002 Conservation of the developmentally regulated dendritic localization of a Purkinje cell-specific mRNA that encodes a G-protein modulator: comparison of rodent and human Pcp2(L7) gene structure and expression. Brain Res. Mol. Brain Res. 105: 1–10. https://doi.org/10.1016/S0169-328X(02)00379-0

Zinyk, D. L., E. H. Mercer, E. Harris, D. J. Anderson, and A. L. Joyner, 1998 Fate mapping of the mouse midbrain-hindbrain constriction using a site-specific recombination system. Curr. Biol. 8: 665–668. https://doi.org/10.1016/S0960-9822(98)70255-6

Communicating editor: J. Schimenti